Integrating transcriptome, physiological, and biochemical studies revealing the role of endogenous ABA and GA 3 in the germination of quinoa seed

Ya Gao
Chengdu University
Chunmei Zheng
Chengdu University
Wenxuan Ge
Chengdu University
Xueying Li
Chengdu University
Xiuzhang Wang
Chengdu University
Wenjun Sun
Chengdu University
Yanxia Sun
Chengdu University
Xiaoyong Wu
cduwxysyx@126.com

Chengdu University

Research Article

Keywords: Quinoa, Seed germination, Abscisic acid, Gibberellic acid, Transcriptome

Posted Date: October 30th, 2024

DOI: https://doi.org/10.21203/rs.3.rs-5283572/v1

Additional Declarations: No competing interests reported.

Abstract

Background

Seed germination, including variations in internal physiological and biochemical indicators, as well as gene expression, has been extensively studied in various plant species. However, there is a lack of significant research attention on the germination mechanisms of quinoa. This study investigated the levels of starch, total amylase, soluble sugars, soluble proteins, glucose, fructose, sucrose, maltose, as well as hormones including ABA and GA_3 during the germination of quinoa seeds. Additionally, enzymatic activities involved in the synthesis and metabolism of ABA and GAs were measured, and transcriptional data at 4 h and 12 h were analyzed to elucidate the internal physiological changes occurring during quinoa germination.

Result

Physiological and biochemical indicators imply that the process of germination involves the enzymatic activity of amylase, which catalyzes the hydrolysis of starch and sucrose. This enzymatic action leads to an increase in the concentrations of soluble sugars, proteins, maltose, and glucose. The enzymes NCED, ZEP, and AAO are involved in the regulation of ABA synthesis, whereas GA_3 levels are modulated by the coordinated activity of GA20ox, GA3ox, and GA2ox. Quinoa seeds exhibit insensitivity to ABA, while GA_3 plays a significant role in promoting seed germination. Transcriptome revealed upregulation of starch and sucrose metabolism and the EMP pathway and TCA cycle were enhanced during seed germination. This study identified 15 crucial genes related to ABA, GAs, starch/sucrose metabolism, and EMP pathway in quinoa germination, via integrated analysis of differential expression, annotations, correlation, and indicator content.

Conclusion

This study investigated the dynamic changes in physiological, biochemical, and energy metabolism indicators during quinoa seed germination by measuring these indicators in conjunction with ABA, GA_3, and transcriptome analysis. Key genes involved in the regulation of quinoa seed germination were identified. The findings provide a foundational theoretical framework for understanding the intrinsic mechanisms underlying quinoa germination and preharvest sprouting.

Introduction

Chenopodium quinoa Wild. is a highly nutritious grain, containing significant amounts of protein, vitamins, minerals, dietary fiber, plant sterols, and phenolic compounds, while also being gluten-free. Additionally, it provides essential amino acids that meeting the human dietary needs. Recognized for its nutritional richness, it is commonly referred to as a "super grain" or "golden grain" [1–4]. Due to its rich

nutritional value, it has been referred to as the perfect and strategic food by Food and Agriculture Organization of the United Nations (FAO) and has the potential to become a substitute for animal protein [5]. Due to the absence of dormancy in quinoa seeds, quinoa is prone to pre-harvest sprouting (PHS) [6, 7].

PHS results in the degradation of proteins, starch, fats, and other essential nutrients in grains, leading to a significant decrease in their nutritional and economic worth [8]. Global data indicates that PHS annually causes economic losses amounting to one billion US dollars [9]. PHS is defined as the occurrence of sprouting in grains while still on the plant, triggered by favorable germination conditions prior to harvest [10]. This phenomenon is intricately linked to seed dormancy and the germination process. Seed germination is a vital stage in the physiological development of crops, playing a critical role in determining quality and yield. It involves a series of orderly physiological and morphological changes that occur following the absorption of water and expansion of seeds [11]. The influencing factors can be categorized into two main groups: external factors such as light, temperature, and water, and internal factors including spike shape, hormones, carbohydrate metabolism, proteinase, reactive oxygen species, seed maturity, and crop variety [12–18]. Seed germination is dependent on the regulation of plant hormones ABA and GAs, as well as the utilization of energy reserves such as starch and soluble sugars.

Research findings have demonstrated the significant roles of plant hormones abscisic acid (ABA) and gibberellic acid (GAs) in the regulation of seed germination and plant maturation [19–21]. The sesquiterpene compound ABA is derived from its precursor, isopentenyl pyrophosphate (IPP), through synthesis in the carotenoid pathway. This process involves a series of enzymes, including Phytoene synthase (PSY), β-carotene hydroxylase (BCH), Zeaxanthin epoxidase (ZEP), Violaxanthin deepoxidase (VDE), 9-cis-epoxycarotenoid dioxygenase (NCED), Short-chain dehydrogenase/Reductase (SDR), and Aldehyde oxidases (AAO) [22]. The degradation of ABA is mediated by hydroxylation reactions catalyzed by P450 cytochrome monooxygenases from the CYP707A family, resulting in a reduction of ABA levels. Specifically, the enzyme responsible for this process is referred to as ABA 8'-hydroxylase (ABA8’-H) [17, 23].

In analogy to ABA, the biosynthetic pathway of GAs is also a complex process. Currently, 136 forms of GAs have been identified and classified into C20 and C19 types based on carbon atom count [24]. Among these forms, only GA_1, GA_3, GA_4, and GA_7 have demonstrated biological activity [25]. The precursor for GAs synthesis is Geranylgeranyl diphosphate (GGPP), and GA_{12} is synthesized through the enzymatic reactions catalyzed by Copalyl diphosphate synthesis (CPS), ent-Kaurene synthesis (KS), ent-Kaurene oxidase (KO), and ent-Kaurenoic acid oxidase (KAO). GA20 oxidase (GA20ox) catalyzes the conversion of GA_{12} into GA_9 and G_{20}, followed by the synthesis of four bioactive GA types, which is catalyzed by GA3 oxidase (GA3ox) [25–30].The deactivation of GAs involves the isomerization of -OH positions in GAs, catalyzed by GA2 oxidase (GA2ox), which plays a crucial role in regulating GAs catabolism [31].

Except for hormones, notable alterations in the content and activity of storage compounds such as starch, protease, amylase, amino acids, and soluble sugars also take place during seed germination [11, 32–36]. Studies in celery [19], soybeans [37], and mustard [38] have demonstrated that significant changes occur in sugar substances during seed germination, leading to enhanced energy metabolism. The utilization of starch and soluble sugars is essential as the primary energy source for seed germination [39].

Currently, there is a scarcity of research that incorporates indicators such as ABA and GAs content, sugar content alterations, and molecular mechanisms in the study of quinoa germination. Transcriptome sequencing includes short-read sequencing, long-read RNA sequencing, and direct RNA sequencing. Illumina, as the primary platform for short-read sequencing, is also the most widely used and mature sequencing platform currently [40] Researchers have used RNA sequencing (RNA-seq) technology to learn gene expression changes during seed germination and identify key germination genes in hazelnut [41], wheat [42], and rice [43].

In this study, Cheng Li (CL-2) was utilized as the material to investigate the mechanism of endogenous physiological and biochemical indicators, as well as gene expression during seed germination. The content of starch, soluble sugar, soluble protein, amylase, maltose, sucrose, fructose, glucose, ABA, GA_3, and the related enzyme activities involved in ABA and GAs synthesis metabolism were quantified. Additionally, transcriptome data obtained at 4-hour and 12-hour time points after germination were analyzed to examine the dynamic changes in various indicators during germination. Moreover, the transcriptome was utilized to evaluate the expression of functionally related genes during the germination of quinoa. This study aimed to elucidate the roles of various markers in the seed germination process and offer valuable insights for further research on quinoa germination.

Materials and methods

Preparation of experimental materials

After a thorough assessment of the germination characteristics and PHS resistance of over 30 quinoa varieties conducted by laboratory members in the preliminary stage, the research concluded that no variety has demonstrated robust PHS resistance as of yet. Nevertheless, variety CL-2 stands out with its high germination rate, making it highly susceptible to PHS. Consequently, CL-2 was chosen as the focal experimental variety for this study. Quinoa CL-2 (Fig. 1), sourced from the Key Laboratory of Coarse Cereal Processing, Ministry of Agriculture and Rural Affairs P.R. China. CL-2 seeds were placed in a culture dish with a filter paper, both with a radius of 4.5 cm, and 6 mL of ultrapure water was added. The aim of this research is to establish a theoretical basis for further exploration into quinoa PHS, achieved through an in-depth study of seed germination. Consequently, the cultivation temperature was set in accordance with the average temperature during the quinoa harvesting season in Chengdu, Sichuan Province, China. The seeds were then placed in an artificial climate box with a light cycle of 14 h at 30℃ followed by a dark cycle of 10 h at 24℃. The humidity was maintained at 50% and the light intensity of

40% for a total duration of 20 h. Experimental samples were collected at intervals of 4, 8, 12, 16, and 20 h, as well as from dry seeds at 0 h. After sampling, the samples were immediately wrapped in tin foil, rapidly frozen in liquid nitrogen, and stored at -80℃ for future use.

Determination of germination rate and water absorption rate

The germination rate was measured according to the Chinese national standard GB SN/T 0800.14–1999. 100 quinoa seeds were randomly selected and then placed on the soaked filter paper in a culture dish. The seeds were placed in the artificial climate box (with the same conditions as mentioned), and the germination data were recorded. Germinated seeds were removed from the culture dish for each record to avoid interference with data statistics, with three biological replicates. The determination of water absorption rate was detailed in prior research study [44].

Measurement of physiological and biochemical parameters

The levels of soluble protein, soluble sugar, and starch content were determined according to the instructions of the assay kits provided by Suzhou Comin Biotechnology Co., Ltd. Furthermore, the level of total amylase activity detected based on the instruction of the assay kit provided by Shanghai yuanye Bio-Technology Co., Ltd. High-performance liquid chromatography (HPLC) was employed to determine the content of fructose, glucose, sucrose and maltose during seed germination. The content of ABA and GA_3 was quantified utilizing the Electron Spray Ionization-High-Performance Liquid Chromatography-Mass Spectrometry/Mass Spectrometry (ESI-HPLC-MS/MS) internal standard method. Enzyme activities for ZEP, NCED, AAO, ABA8'-H, GA20ox, GA3ox, and GA2ox were evaluated employing enzyme-linked immunosorbent assay (ELISA) kits sourced from Jiangsu Meimian Industrial Co., Ltd. Comprehensive details regarding kit models and specific assay methodologies are available in Appendix A. All experiments were performed with three biological replicates.

Transcriptome quality control, sequencing, and analysis process

Based on the experimental results in section 2.2, the timing for collecting samples for transcriptome analysis was determined. Specifically, the cultured seeds were rapidly frozen in liquid nitrogen, followed by RNA extraction and assessment of RNA integrity. The mRNA was enriched using magnetic beads for cDNA library construction, and the library was subsequently assessed for quality. Sequencing by synthesis was then conducted by the Illumina sequencing platform.

Transcriptome sequencing was commissioned to Wekemo Tech Group Co., Ltd. (Shenzhen China). Data quality control (QC) was conducted using Fastp [45], followed by genome alignment performed using HISAT2 [46]. Alignment evaluation was carried out through QualiMap v.2.2.2 dev [47]. Gene count, Fragments Per Kilobase of transcript per Million mapped reads (FPKM) and Transcripts Per Million (TPM) were calculated by Feature Counts [48]. Differentially expressed genes (DEGs) during the

germination process of quinoa seeds were identified based on the criteria of |log2(FoldChange)| > 1 and adjusted p-value < 0.05. Conduct enrichment analysis on fragments utilizing the R language cluster profiler package [49], and annotate DEGs through the Gene Ontology (GO), Kyoto Encyclopedia of Genes and Genomes (KEGG), and STRING databases.

Searching for key genes

The Spearman correlation coefficient of DEGs residing within distinct biological pathways was calculated by the R language. Gene correlations were assessed using a threshold coefficient of ≥ 0.4 and a significance level of $p < 0.05$. Furthermore, the correlation network was visualized by the cytoNCA plugin within the Cytoscape. The computational analysis of pivotal genes was conducted by the utilization of the Cytohubba and MCODE (Degree cutoff = 2, Node score cutoff = 0.2, K-core = 2, and Max depth = 100,) plugins, in conjunction with the STRING database. In the Cytohubba analysis, 9 distinct calculation methods were utilized, including MCC, DMNC, MNC, Degree, Closeness, Betweenness, EPC, Stress, Radiality. In cases where the number of nodes was fewer than 10, the top 5 genes were selected for ranking, whereas for networks with more than 10 nodes, the top 10 genes were chosen.

RNA extract and RT-qPCR

The sample RNA was successfully extracted by following the detailed instructions outlined in the plant tissue extraction kit (Tiangen, Beijing, China). Subsequently, after confirming the RNA's quality through rigorous inspection, cDNA synthesis was carried out in accordance with the instructions provided in the FastKing RT Kit (with gDNase, Tiangen, Beijing, China). Detailed procedures pertaining to RNA quality assessment, cDNA synthesis, and primer design can be found in previous research [44].

The reference gene for RT-qPCR standardization was *ACT* [44]. RT-qPCR was performed by M5 Hiper SYBR Premium EsTaq with Tli RNaseH (MeiBio, Beijing, China). The RT-qPCR reaction mixture included 1 μL of cDNA (80 ng/μL), 0.4 μL of forward primer (100 μM), 0.4 μL of reverse primer (100 μM), 10 μL of 2 × M5 Hiper SYBR Premium EsTaq (containing Tli RNaseH), and RNase Free ddH_2O (adjusted to 20 μL). The RT-qPCR reaction consisted of an initial pre-denaturation step at 95°C for 30 s, followed by denaturation at 95°C for 5 s, and extension at 60°C for 30 s, repeated for 40 cycles. The specificity of primer amplification was validated through a melting curve analysis ranging from 60 to 95°C with a ramp rate of 5°C/s.

Data processing and analysis

The experimental data were curated using Excel 2016. ANOVA and correlation analysis were conducted using IBM SPSS Statistics 26. Graphical representations were created by Graph Pad Prism 8, Origin Pro 2023, Cytoscape, and Adobe Illustrator 2023.

Result

Changes in seed water absorption and germination rate

The germination rate of CL-2 seeds over a 48-hour period (Fig. 2) displayed a gradual increase from 0 to 20 h, with no statistically significant changes observed thereafter until 48 h ($p > 0.05$). As a result, the optimal time for sampling biochemical indicators in the later stage was determined to be at the 20-hour mark. The germination rate exhibited relatively low levels during the initial 0–8 h, referred to as the "germination preparation stage", followed by the 8–20 h characterized as the "germination stage", and the subsequent 8–16 h designated as the "rapid germination stage". After 20 h, the average germination rate of seeds reached 95%, suggesting optimal seed viability. The findings regarding seed water absorption rate (Fig. 2) demonstrated a swift uptake of water by the seeds within the initial 4 hours, labeled as the "rapid water absorption stage", followed by a gradual and consistent water absorption starting at 8 h.

Changes of storage compounds during seed germination

A reduction in starch content was observed during the germination process of seeds, as illustrated in Fig. 3. The highest starch content, recorded at 519.85 ± 13.14 mg/g, was observed in 0-hour. Following 20 h of germination, the starch content decreased to its lowest point, measuring at 208.66 ± 40.19 mg/g. Changes in total amylase activity were also depicted in Fig. 3. During the rapid water absorption stage (0–4 h), amylase activity peaked at 6.70 ± 0.62 U/L. Subsequently, there was a decline in amylase activity, with the enzyme activity reaching its minimum at 2.12 ± 0.42 U/L after 20 h. The soluble protein content demonstrated a decrease from 0 h to 12 h, followed by a subsequent overall increase in the later stages. Specifically, at the 12-hour mark, the minimum value observed was 8.13 ± 2.62 mg/g, which subsequently peaked at 39.96 ± 2.79 mg/g by the 16-hour mark. In contrast, the soluble sugar content exhibited a decline during the initial 0–8 h period, followed by a rapid increase from 8 h to16 h, and a subsequent decrease after 16 h. The minimum and maximum soluble sugar content values were recorded at 14.86 ± 1.12 mg/g and 32.64 ± 4.85 mg/g, respectively, at 4 and 16 h.

Changes of small molecule sugar content during seed germination

The results of analyzing fructose, glucose, sucrose, and maltose levels during the germination process of quinoa seeds are presented in Fig. 4. In terms of the sugars analyzed, fructose displayed the lowest content, fluctuating within a narrow range of 0.335 to 0.358 mg/g. In contrast, glucose levels showed an upward trend during the initial stages of germination (0–8 h), indicating a consistent increase in concentration over time. When compared to monosaccharides, disaccharides demonstrated higher levels, specifically maltose with a distribution spanning from 2.52 to 3.474 mg/g and sucrose distribution ranging from 1.177 to 3.22 mg/g. The maximum value of maltose content was observed at 8 h. Sucrose, on the other hand, was higher in dry seeds but underwent a marked decline throughout the germination process.

Changes in ABA and GA_3 during germination process

The results of ABA and GA_3 content within 20 h of seed germination are depicted in Fig. 5. A notable pattern was observed in the ABA content, showing an increase followed by a decline at the 12-hour mark. The lowest ABA content was detected in the dry seeds, measuring at 2.33 ± 0.27 ng/g, whereas the peak level was recorded at 12 h, reaching 6.20 ± 0.26 ng/g. Statistical analysis indicated a significant difference in ABA content at 0 h, 4 h, and 8 h ($p < 0.05$), with no significant disparity observed between the subsequent time intervals from 8 to 20 hours ($p > 0.05$). On the contrary, the GA_3 content in the dry seeds was observed to be at its lowest level (0.05 ± 0.02 ng/g), during the stage of rapid water absorption by the seeds, at the 4-hour mark, the GA_3 concentration reached its peak at 1.64 ± 0.27 ng/g before experiencing a sharp decline. Between the 8 to 20-hour time interval, the GA_3 content fluctuated within the range of 0.04 to 0.65 ng/g.

Changes in ABA and GAs-related enzyme activity

The results of hormone-related enzyme activity are illustrated in Fig. 6. The enzyme activity linked to ABA synthesis exhibited the lowest value in the dry seeds, with ZEP, NCED, and AAO showing minimum enzyme activities of 998.91 ± 20.01 U/L, 491.92 ± 6.81 U/L, and 40.43 ± 0.87 U/L, respectively. Subsequently, during the rapid germination stage of seeds, the enzyme activity peaked at 16 h, 16 h, and 12 h, respectively, with values of 1194.87 ± 13.33 U/L, 625.77 ± 10.11 U/L, and 44.93 ± 0.52 U/L. The ABA synthase ZEP demonstrated the highest level of activity, ranging from 979.39 to 1210.35 U/L, while the AAO enzyme exhibited the lowest activity, with a range of 39.49 to 45.68 U/L. The ABA8'-H enzyme, which mediates ABA decomposition, exhibited consistent activity during the germination preparation phase, followed by a rapid increase and subsequent decline around the 16-hour mark.

The expression levels of GA20ox and GA3ox, key enzymes involved in GAs synthesis, exhibited a consistent upward trajectory during seed germination, as depicted in Fig. 7. In the dry seeds, the enzymatic activities of GA20ox and GA3ox were relatively low at 194.33 ± 4.66 U/L and 47.97 ± 0.85 U/L, respectively. Subsequently, from 8 h to 20 h post-germination, the enzymatic activities of both synthases increased steadily, reaching maximum values of 222.94 ± 3.70 U/L and 61.46 ± 0.91 U/L for GA20ox and GA3ox, respectively. The activity of GAs metabolic enzyme GA2ox displayed a biphasic pattern, with an initial increase followed by a decline, reaching a maximum value of 21.55 ± 0.34 U/L at 16 h. The lowest activity of GA2ox was observed in the dry seeds, registering at 17.33 ± 0.09 U/L.

Illumina sequencing and quality control

Based on the experimental results of germination rates, we observed that 8 h marked a turning point in germination. Prior to 8 h, the germination rate was relatively low. However, once exceeding this point, the seed germination rate accelerated significantly. Based on this finding, time points before and after 8 h (specifically, 4 h and 12 h) were decided to be selected as comparisons for pre- and post-germination stages. Quinoa seeds underwent a germination period of 4 h for the control group and 12 h for the experimental group. The specifics of the sequencing samples after QC are presented in Table 1.

Following QC, the data volume of clean data per sample ranged from 6.04 GB to 6.47 GB, with an overall comparison rate of 96.70–97.50%. The Q30 ratio ranged from 92.44–93.12%, and the GC content varied from 43.69–44.85%. These results confirm the reliability of the transcript data and the use of clean data for further analyses.

Table 1
Sequence information after quality control

Sample ID	Before QC	After QC	Q20 rate	Q30 rate	GC content	Overall mapping rate
4h-01	6.78G	6.47G	97.71%	93.12%	44.78%	97.50%
4h-02	6.42G	6.12G	97.57%	92.86%	44.48%	97.40%
4h-03	6.6G	6.27G	97.38%	92.44%	44.85%	97.20%
12h-01	6.32G	6.04G	97.55%	92.80%	43.69%	97.40%
12h-02	6.35G	6.07G	97.61%	92.96%	44.07%	96.70%
12h-03	6.43G	6.13G	97.47%	92.62%	44.07%	97.20%

Furthermore, by assessing the correlation between samples using TPM data, the reproducibility of biological experiments within the sample group was evaluated. The Spearman correlation coefficient analysis revealed that coefficients greater than 0.92 indicate a strong correlation between samples, as depicted in Fig. 8.

DEGs analysis by GO annotation

By utilizing the criteria of |log2(FoldChange)| > 1 and padj < 0.05 to identify DEGs, a total of 3349 DEGs were identified in the comparison between 4 h and 12 h; of these, 2113 DEGs exhibiting upregulation and 1236 DEGs showing downregulation (Fig. 9). The functional annotation of DEGs within specific pathways was performed using GO, resulting in a total of 3030 GO entries. These entries encompassed 2132 biological processes, 595 molecular functions, and 303 cellular components. A total of 15686 genes were associated with these GO entries, specifically including 1588 DEGs included. The p-values associated with these annotations were adjusted using the false discovery rate (FDR) method.

In the top 20 most significant entries of GO analysis (Fig. 10A), the focus is on Response, Hydrolase, Circadian, and Biosynthetic. The top 5 significant biological processes include Seed maturation (0010431), Sterol metabolic process (00016125), Multicellular organismal homeostasis (00048871), Sterol biosynthetic process (0016126), and Response to water (00009415). In terms of molecular functions, the most significant entries are Cysteine-type endopeptidase activity (0004197), Hydrolase activity and acting on glycosyl bonds (0016798), Hydrolase activity and hydrolyzing O-glycosyl compounds (0004553), and Acid phosphatase activity (0003993).

Among statistically significant GO terms (padj < 0.05), which pertaining to seed germination and maturation, entries included Seed maturation (0010431), Regulation of seed germination (0010029),

Rhythmic process (0048511), Positive regulation of seed germination (0010030), and Regulation of seedling development (1900140). Notably, only the "Response to gibberellin" (0009739) within the GAs and ABA relative GO entries demonstrated statistical entries showed significance, with an adjusted p-value of 0.0543. In the carbohydrate-related GO entries, Carbohydrate catabolic process (0016052) exhibited statistical significance with an adjusted p-value of 0.0447.

DEGs analysis by KEGG annotation

To further investigate the DEGs expression profiles, the DEGs were annotated by the KEGG database. A total of 13242 genes were enriched in 365 KEGG pathways, including 1639 DEGs. The findings presented in Fig. 10 (B) illustrate the top 20 pathways with the lowest adjusted p-values, suggesting a notable enrichment in pathways associated with carbon metabolism, plant hormone signaling, biosynthesis of biologically active compounds, and lipid-related processes. To further elucidate the alterations in starch, sugar, ABA, and GA_3 levels, as well as signaling pathways related to ABA and GAs during quinoa seed germination, an extensive annotation analysis of the KEGG pathways was conducted.

The result revealed that the ABA synthesis metabolic pathway (M00372) did not show statistically significant enrichment ($p > 0.05$), while the Diterpenoid biosynthesis pathway (ko00904), including the GAs biosynthetic pathways M00927, M00928, and M00929, displayed significant enrichment ($p < 0.05$). Furthermore, the Plant hormone signal transduction pathway (ko04075) exhibited highly significant enrichment ($p < 0.001$). The expression levels of DEGs, as measured by Fragments Per Kilobase Million (FPKM) and Fold Change (FC), related to the ABA and GAs pathways are illustrated in Fig. 11.

In the realm of hormone synthesis metabolism, the ABA pathway consists of a total of 21 genes, among which 5 genes, namely *ZEP_1*, *ZEP_2*, *CYP707A*, *ABA2*, and *LUT5*, were identified as DEGs (The full names and IDs corresponding to the abbreviations of genes are detailed in Appendix B.). The FC for ABA biosynthesis genes varied from − 1.68 to 1.22 overall, with *ZEP* and *LUT5* showing downregulation in expression, while *ABA2* exhibited upregulation. Notably, the metabolic gene *CYP707A* displayed significant downregulation, with a FC of -3.25. Meanwhile, the pathways related to ABA and GAs were exhibited in Fig. 12.

Furthermore, a total of 21 genes have been identified as being associated with GAs, with 7 of these genes identified as DEGs: *CYP701_1*, *CYP701_2*, *GA3ox*, *KAO*, *GA20ox*, *GA2ox_1*, and *GA2ox_2*. Specifically, genes *GA2ox_1*, *GA2ox_2*, and *KAO* exhibited significant upregulation during germination, while *CYP701_1*, *CYP701_2*, *GA3ox*, and *GA20ox* showed significant downregulation. The observed upregulation of the upstream GAs synthesis gene *KAO* (FC = 2.96) and the downregulation of *CYP701_1*, *CYP701_2*, *GA20ox*, and *GA3ox* (with FC ranging from − 1.60 to -1.01) suggest a regulatory role in GAs synthesis. Noteworthy is the differential expression of DEGs of *GA2ox* in quinoa, specifically *GA2ox_1* and *GA2ox_2*, with FC of 4.69 and 4.85, respectively.

Additionally, 48 genes are involved in the ABA signaling pathway and 13 genes in the GAs signaling pathway within the broader context of plant hormone signaling pathways. Among these, 14 DEGs were

identified as ABA signaling genes, including *SnRK2_1*, *SnRK2_2*, *PP2C_1*, *PP2C_2*, *PP2C_3*, *PP2C_4*, *ABF_1*, *ABF_2*, *ABF_3*, *ABF_4*, *ABF_5*, *PYL_1*, *PYL_2*, and *PYL_3*. Significantly, a total of 10 genes, including *ABF*, *PYL*, and *SnRK2*, showed upregulation, while *PP2C* displayed downregulation. Moreover, two DEGs, namely *GID1_1* and *GID1_2*, were identified within the GAs signaling pathways, with *GID1_2* being upregulated and *GID1_1* being downregulated.

The starch and sucrose metabolism pathway (ko0050) exhibited significant enrichment, encompassing a total of 236 genes, of which 57 were identified as DEGs (Fig. 13). The schematic representation of the starch and sucrose metabolism process is depicted in Fig. 14, demonstrating the breakdown of sucrose into D-fructose and D-glucose by *INV* and *malZ*, as well as the interconversion of sucrose with UDP-glucose by *SUS* genes. Four homologous *SUS* genes were identified in quinoa, with *SUS*_1 and *SUS_2* showing upregulation by 4.27 and 1.69 times, respectively, while *SUS_3* and *SUS_4* downregulated, with FC of -1.56 and − 1.84, respectively. In quinoa, four homologous genes of *INV* were identified among DEGs, with the highest FC of 4.12. The expression levels of the genes involved in D-fructose degradation metabolism, such as *HK* and *scrk* were concurrently upregulated.

In addition to the breakdown of sucrose into glucose and maltose by *malZ*, and cellulose into glucose by *EGLU* and *β-glu*, a total of 8 *EGLU* homologous genes and 8 *β-glu* homologous genes were identified in quinoa. Among these, only *EGLU_8* showed downregulation with an FC of -1.93. Quinoa also possesses 6 homologous genes of *β-glu*, all of which were upregulated.

Simultaneously, starch undergoes enzymatic catalysis by AMY to produce maltose, while AMY is also involved in the hydrolysis of starch into dextrin. The levels of expression for both *beta AMY* and *alpha AMY* were elevated. In the process of starch biosynthesis, D-glucose-1P is converted into ADP glucose by *glgC*, subsequently leading to the formation of amylose through the activity of the starch synthase gene *glgA*, resulting in starch formation under the influence of *GBE1*. The expression levels of *glgC* and *glgA* increased during germination, whereas the expression of *GBE1* decreased with an FC of -1.16.

The analysis revealed that 161 genes were involved in the glycolysis/gluconeogenesis pathway (ko00010), with 34 DEGs identified (Fig. 15). The genes involved in the glycolysis/gluconeogenesis pathway are presented in Fig. 16. In the initial phase of glycolysis, commonly known as the "energy consumption phase," glucose phosphorylation facilitated by *GALM* and *HK* results in the production of α-D-glucose-6-phosphate. Subsequently, α-D-glucose-6P was isomerized to β-D-fructose-6P and further phosphorylated to generate β-D-fructose 1,6-bisphosphate through the actions of *PFKA* and *PFP*. *PFKA* encodes a crucial enzyme that regulates the rate of glycolysis, and in quinoa, 4 homologous genes (*AUR62031952*, *AUR62033274*, *AUR62039818*, *AUR62005870*) were identified. Among these, only *AUR62005870* exhibited downregulation, with a FC of -1.2.

The enzyme ALDO facilitated the condensation of a six-carbon molecule into two three-carbon compounds, glycerone-P and D-glyceraldehyde 3-P. These three-carbon compounds can be interconverted by the gene *TPI*. In the second stage of glycolysis, referred to as the "energy -yielding stage," the conversion of three-carbon compounds into 3-phospho-D-glyceroyl phosphate by the gene

gapA. Subsequently, the enzymes *MINPP1*, *PK_1*, and *PK_2* facilitated the production of pyruvate, ultimately completing the glycolytic pathway.

Pyruvate was further metabolized through anaerobic oxidization to lactate by *LDH*, or alternatively underwent decarboxylation to generate Acetyl CoA and ethanol, among others byproducts. Acetyl CoA then entered the Tricarboxylic acid cycle (TCA cycle) for further energy production. The process of pyruvate salt formation was facilitated by enzymes including *PDHB*, *NAPH+*, *FRMA*, *ACSS1_2*, and *ALDH*. Notably, the expression levels of *ACSS1_2*, *FRMA*, and *PDHB* were increased, whereas *NADPH +* levels were decreased.

Results of Key genes

Utilizing the R language and Cytoscape, betweenness centrality was computed to identify pivotal genes within the target pathway. Out of the 28 nodes encompassed in the ABA and GAs-related pathways, the top 3 genes were identified as *SnRK2_1*, *GA2ox_2*, *ABF_2* (Fig. 17). Additionally, the associations between starch and sucrose metabolism pathways and glycolysis pathways individually assessed, leading to the establishment of networks for the top 30 correlated nodes within these pathways (Fig. 18 and Fig. 19). The findings revealed that *malZ_2*, *glgA_2*, and *SUS_3* were the top 3 ranked genes in the starch and sucrose metabolism pathway, while *PDHB_2*, *ALDH_1*, and *HK* were the top 3 in the glycolysis pathway.

Based on the rankings provided by 9 different computation methods in Cytohubba, the intersection of genes ranked by these diverse methods was chosen, and these genes were designated as the central genes calculated by Cytohubba's computation. The results showed that *GA3ox*, *GA20ox*, *ABA2*, *CYP707A*, and *ZEP* as central genes in the ABA and GAs-related gene pathways. However, in the realm of starch and sucrose metabolism, a total of 5 central genes were identified: *SUS*, *PYG*, *GBE1*, *PGM*, and *HK*. In the context of glycolysis, the genes *LDH*, *PGM*, ALDO, *PFKA*, *NAPH+*, *PK*, and *TPI* were identified. The specific computational findings are outlined in Appendix C.

The key parameters for central network analysis were determined by the MCODE algorithm. Subsequent analysis revealed the significance of *PP2C*, *ZEP*, *ABA2*, *CYP707A*, and GA2ox in the ABA and GAs-related pathway, as illustrated in Fig. 20. Similarly, *SUS*, *scrk*, *PGM*, alpha AMY, *HK*, ostB, *GBE1*, *INV*, and *PYG* were identified as central network genes in the starch and sucrose metabolism pathway. In glycolysis, the genes *HK*, *PGM*, *NAPH+*, *PFKA*, *LDH*, *PK*, ALDO, and *TPI* were identified as central networks.

By examining DEGs functions, pre- and post-germination FC, gene correlations, and the central networks extraction, key genes from various pathways were identified. Subsequent analysis revealed key genes involved in the ABA and GAs pathways, including *CYP707A* (*AUR62001756*), *ABA2* (*AUR62021168*), *GA2ox_1* (*AUR62024597*), and *GA2ox_2* (*AUR62011753*). In the pathway of starch and sucrose metabolism, pivotal genes were identified, including *INV_1* (*AUR62009834*), *INV*_2 (*AUR62039932*), *malZ_1* (*AUR62021097*), *beta glu_6* (*AUR62029347*), *EGLU_1* (*AUR62000202*), *EGLU_2* (*AUR62006550*),

scrk_1 (*AUR62002325*), *HK* (*AUR62031934*), and *alpha AMY* (*AUR62012986*). Similarly, essential genes involved in glycolysis were *HK* (*AUR62031934*), *ACSS_1* (*AUR62032527*), and *ACSS_2* (*AUR62017459*).

RT-qPCR validation

Based on the results of Cytohubba calculations, gene correlation analysis, gene variation multiples, and a thorough literature review, a total of 15 DEGs were chosen for further validation through RT-qPCR analysis in pathways associated with diverse biological processes, with the primer sequences detailed in Appendix D. (Fig. 21). The results demonstrated that the expression trends observed in the RNA-seq results were consistent with the calculated expression levels obtained from RT-qPCR.

Discussion

Excessive consumption of compounds during seed germination

Upon contact with water, seed germination entails the utilization of reserves and the provision of energy, which leads to the prompt initiation of internal physiological mechanisms such as protease activation and signal transmission [50, 51]. In this study, the seeds demonstrated substantial water absorption within the first 4 h, accompanied by a rapid increase in total amylase activity that reached its maximum value. The germination of CL-2 was accompanied by a significant decrease in starch content, which was attributed to enzymatic hydrolysis catalyzed by amylase, leading to the formation of soluble sugars like maltose and glucose. Starch, as the main internal component in plants, acts as a key energy store and is crucial for various physiological processes necessary for plant growth and development[52].

In the process of germination, there was a notable elevation in maltose and glucose content, along with an increase in soluble sugars, while the alteration in fructose content was relatively minor. In quinoa, study had indicated a consistent reduction in starch levels throughout seed germination, accompanied by elevated levels of fructose and glucose compared to dry seeds, followed by a subsequent decrease after an initial surge [53]. Similarly, during the in vitro germination of *Dendrocalumus brandisii*, there was a continuous decrease in starch content, coupled with an increase in soluble sugars [54]. In our study, a consistent decline in sucrose content was observed during the germination, with a minor increase noted in the later stages, showing similar findings on quinoa before [53].

Changes in content are closely associated with gene regulatory processes. Transcript analysis indicated the genes *SUS*, *INV*, and *malZ*, which facilitate the conversion of sucrose into fructose and glucose, showing differing levels of upregulation at 4 h to 12 h. By utilizing a combination of FC and gene correlation analysis, it was determined that *INV_1*, *INV_2*, and *malZ_1* play a crucial role in the breakdown of sucrose content during the 4 h to 12 h germination process. Within the pathway of starch and sucrose metabolism, *beta glu*, *EGLU*, *otsB*, *TPS*, *TREH*, and *GN* act as intermediaries in glucose production, with *beta glu_6*, *EGLU_1*, and *EGLU_2* identified as key genes in glucose synthesis during CL-2 germination.

In the pathway of fructose metabolism, *HK* and *scrk*_1 have been identified as key contributors, and their upregulation plays a significant role in promoting fructose metabolism. Additionally, the limited fluctuations in fructose levels during germination may be linked to the continuous degradation of sucrose. The upregulation of amylase genes, specifically *alpha AMY* and *beta AMY*, results in a rise in maltose levels and a corresponding decrease in starch levels. Under the guidance of the *ISA*, *alpha AMY* and *beta AMY* facilitate the breakdown of starch into maltodextrin and dextrin, with maltodextrin subsequently converting into maltose through the action of amylase.

Enhanced sugar metabolism during seed germination

The majority of genes within the EMP pathway demonstrated marked upregulation, particularly those responsible for the key rate-limiting steps in EMP pathway, encoding hexokinase (*HK*), phosphofructokinase (*PFKA_1*, *PFKA_2*, *PFKA_3*), and pyruvate kinase (*PK_1*, *PK_2*, *PK_3*). Furthermore, the TCA cycle also exhibited significant gene enrichment, with a total of 10 DEGs identified in the cycle. Particularly noteworthy were the upregulation of key genes responsible for the three rate-limiting reactions of the TCA cycle, including citrate synthase genes *ACLY_1* (*AUR62039280*), *ACLY_2* (*AUR62014075*), and *ACLY_3* (*AUR62005413*); isocitrate dehydrogenase gene *IDH* (*AUR62018235*); and α-ketoglutarate dehydrogenase genes *OGDH_1* (*AUR62029475*) and *OGDH_2* (*AUR62003361*).

The citrate synthase gene family displayed the largest FC, with *ACLY_1* exhibiting a FC of 2.98, *ACLY_3* with a FC of 3.00, and *ACLY_2* with a FC of 1.71. In addition to the EMP pathway and the TCA cycle, other sugar metabolism pathways such as the pentose phosphate pathway did not show significant differences during CL-2 seed germination. In conclusion, the energy necessary for seed germination is supplied through sugar metabolism, specifically via the EMP pathway, pyruvate oxidation, and the TCA cycle.

ABA accumulation during seed germination under enzyme action

Based on the findings of the analysis of ABA and its associated enzymes activities, it was noted that the activities of ABA synthetic enzymes ZEP, NCED, and AAO exhibited a notable increase following seed germination, aligning with the observed fluctuations in ABA content. Further examination through correlation analysis indicated a statistically positive relationship (Appendix E.).

The findings indicated no consistent correlation between the transcriptional levels of genes encoding ZEP, NCED, AAO, and ABA8’-H and protease activity. According to the central dogma of molecular biology [55], gene expression involves a sequential process of DNA transcription, mRNA translation, and protein synthesis. Previous research [56, 57] has shown that various post-transcriptional mechanisms, such as processing, degradation, translation, and modifications, are essential for the activation of transcripts into functional proteins. Although transcriptional abundance can be indicative of protein expression levels, the correlation between the two is not always definitive. Post-translational modifications (PTMs) of protein are widely acknowledged as significant factors that impact protein accumulation and

functionality. These modifications, such as methylation, ubiquitination, acetylation, sumoylation, persulfidation, as well as phosphorylation and dephosphorylation [58–62], play crucial roles in regulating protein activity. Studies on cucumber [63] and triple-negative breast cancer [64] has indicated that variations in post-translational modification states can result in discrepancies between protein and transcriptional levels due to post-translational ubiquitination modifications.

Various modification methods, such as sumoylation and phosphorylation, have been reported in the regulation of phytohormones, with *SnRK2.6* being influenced by these modifications [58]. Simultaneously, the biological activity of Abscisic acid-insensitive 5 (ABI5) relies on phosphorylation and ubiquitination modifications [65, 66]. In addition to the ABA signaling pathway, various phytohormones, including *DELLA* in GAs [67], *AHP6* in cytokinin [68], *CTR1* in ethylene [69], and *BIN2* in Brassinosteroids(BR) [70], participate in PTMs that regulate their bioactivity. Hence, it was deduced that the discrepancy between the transcriptional regulation of target genes and enzyme activity within the ABA biosynthesis pathway could potentially be influenced by biological mechanisms such as transcriptional processing and PTMs.

The content of ABA is a result of the combined effects of multiple genes [71, 72]. Notably, DEGs including *ZEP*, *LUT5*, *ABA2*, and *CYP707A* were identified within the ABA biosynthetic pathway. Specifically, the results of this study indicated a significant upregulation of *ABA2* and a marked downregulation of *CYP707A*. It can be inferred that the accumulation of ABA between 4 and 12 h is primarily regulated by the coordinated activity of *ABA2* and *CYP707A*. Furthermore, the expression profiles of ABA-related genes identified in this research align with previous white quinoa (BL) sequencing data (RNA seq data available at http://trace.ncbi.nlm.nih.gov/Traces/sra, PRJNA590581) [73].

In the hormone signaling pathways, *PYL*, *SnRK2*, and ABF were identified as upregulated genes, while PP2C expression was downregulated, resulting in negative regulation of seed germination. The observed gene expression pattern in BL [73]was found to be consistent with that of CL-2 in this study.

Despite the traditional understanding of ABA as a suppressor of seed germination [17], previous studies on quinoa have showed that seeds with lower dormancy levels have higher endogenous ABA levels [74]. This indicates that the endogenous ABA content in quinoa may not be directly associated with dormancy. Moreover, diverse cultivars of quinoa demonstrate differential responses to ABA at different stages, with seeds exhibiting reduced sensitivity to ABA during dormancy release and heightened sensitivity to GAs signaling [75]. Additionally, researchers [74] suggested notable disparities in the quinoa germination efficiency attributed to variations in sowing timing and seed coat thickness. Similarly, analysis of 189 quinoa materials using phenotype modeling indicated that 141 of the materials did not exhibit primary dormancy, and revealed a correlation between seed coat thickness, eccentricity, and quinoa dormancy and germination [76]. Overall, the growing body of research on quinoa indicates that its germination traits are impacted by various factors, with ABA content potentially not playing a direct role.

GAs plays a positive regulatory role in seed germination process

GAs has been identified as a crucial phytohormone involved in the regulation of seed germination, root and stem elongation, and cell elongation [77]. The rapid uptake of water leads to an increase in GA_3 levels, indicating a strong relationship between seed moisture content and GA_3 levels. Following-germination, there is a notable rise in GA_3 content in quinoa seeds, similar to the process observed in the release of dormancy wheat (*Triticum aestivum L.*) seeds [78], Japanese apricot seeds (*Prunus mumeSieb. et Zucc*) [79] ,and tomato seeds [80]. Notably, in quinoa seeds, there is a rapid increase in GA_3 levels within the first 4 hours of germination, followed by a decrease at the 4-hour mark, and subsequently, a sustained minor fluctuation in GA_3 levels from 8 h to 20 h. Previous study on cotton (*Gossypium hirsutum L.*) [81] has demonstrated a similar pattern of GA_3 levels peaking and subsequently declining during seed germination, whereas in grapes [82], GAs levels decrease during the transition from dormancy induction to maintenance and release. As a result, during the germination of quinoa seeds, there is a simultaneous production and utilization of endogenous GA_3, with consumption rates being lower than synthesis rates, leading to a trend in GA_3 levels during the process.

The enzymes GA20ox and GA3ox play key roles in converting inactive forms of GAs into active GAs, while GA2ox is responsible for GAs deactivation [83, 84]. Analysis of enzyme activity demonstrated an increase in synthesis enzyme activity following seeds germination, promoting the accumulation of GAs. The activity of GA2ox initially increased during the early stages of germination, followed by a decline in the later stages, which suggests GA2ox plays a key role in regulating GAs homeostasis. The lack of significant correlation between GA_3 and the activities of GA20ox, GA3ox, and GA2ox implies that this observation may be attributed to the presence of various active forms of GAs, including GA_1, GA_3, GA_4, and GA_7 [85].

The integrated transcriptional results and correlation analysis indicated that the decrease in GA_3 content at 4 h compared to 12 h is primarily attributed to the downregulation of *GA2ox_1* and *GA2ox_2*. Report have shown that the overexpression of *GA2ox* results in plants displaying GA-deficient phenotypes [24]. In maize subjected to cold and drought stress, the expression levels of GA2ox were found to be inversely related to GAs content [86]. Numerous studies have demonstrated the significant involvement of GA2ox in the regulation of GAs metabolism. Despite the upregulation of the upstream GAs synthesis gene *KAO*, the coordinated activity of *CYP701_1*, *CYP701_2*, *GA20ox*, *GA3ox*, *GA2ox_1*, and *GA2ox_2* results in a reduction in GA_3 content. Notably, *GA2ox_1* and *GA2ox_2* play pivotal roles in modulating the GAs pathway.

Conclusions

The study conducted an experiment to analyze the content of endogenous physiological and biochemical indicators during different stages of quinoa seed germination. By integrating the findings from the 4-hour and 12-hour transcriptome analyses, the study investigated the dynamic changes in physiology and transcription levels. The results indicated that starch and sucrose played a crucial role in providing energy for seed germination, leading to an overall increase in levels of soluble sugars, soluble proteins, and small-molecule sugars such as glucose and maltose.

Enzymes including ZEP, NCED, and AAO play a crucial role in the regulation of ABA synthesis, resulting in an increase in endogenous ABA content during seed germination. The study suggests that the relationship between the endogenous ABA content and germination status in quinoa may not be definitive. The activity of GA20ox, GA3ox, and GA2ox enzymes collectively governs the content of GA_3, which, in turn, facilitates seed germination. The analysis of the transcriptome revealed 3349 DEGs, with KEGG annotation indicating enhanced activity in hormone signaling, starch and sucrose metabolism, the EMP pathway, and the TCA cycle. This study investigated the mechanisms underlying quinoa germination at physiological and genetic levels, thereby laying a theoretical foundation for future investigations on quinoa seeds.

Declarations

Ethics approval and consent to participate

Not applicable.

Availability of data and materials

The RNA-seq data generated and analyzed for this study are available at NCBI in BioProject ID PRJNA1028334.

Competing interests

The authors declare that they have no competing interests.

Funding

This work was supported by the Sichuan Province Science and Technology Program (Grant Number: 2022YFQ0041); the Project of Sichuan Provincial Administration of Traditional Chinese Medicine (Grant Number: 2023MS273).

Acknowledgements

The authors acknowledge the support of the Key Laboratory of Coarse Cereal Processing, Ministry of Agriculture and Rural Affairs P.R. China.

References

1. Hussain MI, Farooq M, Syed QA, Ishaq A, Al-Ghamdi AA, Hatamleh AA. Botany, nutritional value, phytochemical composition and biological activities of quinoa. Plants 2021, 10(11):2258.
2. Pathan S, Siddiqui RA. Nutritional composition and bioactive components in quinoa (Chenopodium quinoa Willd.) greens: A review. Nutrients 2022, 14(3):1–12.
3. Filho AM, Pirozi MR, Borges JT, Pinheiro Sant'Ana HM, Chaves JB, Coimbra JS. Quinoa: Nutritional, functional, and antinutritional aspects. Crit reviews food Sci Nutr 2017, 57(8):1618–30.
4. Tabatabaei I, Alseekh S, Shahid M, Leniak E, Wagner M, Mahmoudi H, Thushar S, Fernie AR, Murphy KM, Schmöckel SM, et al. The diversity of quinoa morphological traits and seed metabolic composition. Sci Data. 2022;9(1):1–7.
5. Dakhili S, Abdolalizadeh L, Hosseini SM, Shojaee-Aliabadi S, Mirmoghtadaie L. Quinoa protein: composition, structure and functional properties. Food Chem 2019:125161.
6. Lopes CO, Barcelos MFP, Vieira CNG, de Abreu WC, Ferreira EB, Pereira RC, de Angelis-Pereira MC. Effects of sprouted and fermented quinoa (Chenopodium quinoa) on glycemic index of diet and biochemical parameters of blood of Wistar rats fed high carbohydrate diet. J Food Sci Technol. 2019;56:40–8.
7. Ceccato DV, Bertero HD, Batlla D. Environmental control of dormancy in quinoa (Chenopodium quinoa) seeds: two potential genetic resources for pre-harvest sprouting tolerance. Seed Sci Res. 2011;21(2):133–41.
8. Vetch JM, Stougaard RN, Martin JM, Giroux MJ. Revealing the genetic mechanisms of pre-harvest sprouting in hexaploid wheat (Triticum aestivum L). Plant Sci. 2019;281:180–5.
9. Tai L, Wang H-J, Xu X-J, Sun W-H, Ju L, Liu W-T, Li W-Q, Sun J, Chen K-M. Pre-harvest sprouting in cereals: genetic and biochemical mechanisms. J Exp Bot. 2021;72(8):2857–76.
10. Nakamura S. Grain dormancy genes responsible for preventing pre-harvest sprouting in barley and wheat. Breed Sci 2018, 68(3):295–304.
11. Guardianelli LM, Salinas MV, Brites C, Puppo MC. Germination of white and red quinoa seeds: improvement of nutritional and functional quality of flours. Foods 2022, 11(20):1–18.
12. Rabieyan E, Bihamta MR, Moghaddam ME, Mohammadi V, Alipour H. Genome-wide association mapping and genomic prediction for pre–harvest sprouting resistance, low α-amylase and seed color in Iranian bread wheat. BMC Plant Biol. 2022;22(1):300.
13. Tai L, Wang HJ, Xu XJ, Sun WH, Ju L, Liu WT, Li WQ, Sun J, Chen KM. Pre-harvest sprouting in cereals: genetic and biochemical mechanisms. J Exp Bot. 2021;72(8):2857–76.
14. Barrero JM, Porfirio L, Hughes T, Chen J, Dillon S, Gubler F, Ral JF. Evaluation of the impact of heat on wheat dormancy, late maturity α-amylase and grain size under controlled conditions in diverse germplasm. Sci Rep. 2020;10(1):17800.
15. Javaid MM, Mahmood A, Alshaya DS, AlKahtani MDF, Waheed H, Wasaya A, Khan SA, Naqve M, Haider I, Shahid MA, et al. Influence of environmental factors on seed germination and seedling

characteristics of perennial ryegrass (Lolium perenne L). Sci Rep. 2022;12(1):9522.
16. Klupczyńska EA, Pawłowski TA. Regulation of seed dormancy and germination mechanisms in a changing environment. Int J Mol Sci 2021, 22(3):1–13.
17. Ali F, Qanmber G, Li F, Wang Z. Updated role of ABA in seed maturation, dormancy, and germination. J Adv Res 2022:199–214.
18. Li H, Li X, Wang G, Zhang J, Wang G. Analysis of gene expression in early seed germination of rice: landscape and genetic regulation. BMC Plant Biol. 2022;22(1):1–12.
19. Li H, Chen J, He L, Zhu H, Huang Z, Zhu M, Fan L, Wu L, Yu L, Zhu W, et al. Transcriptome analyses reveal the role of light in releasing the morphological dormancy of celery seed by integrating plant hormones, sugar metabolism and endosperm weakening. Int J Mol Sci. 2022;23(17):1–12.
20. Barreto LC, Herken DMD, Silva BMR, Munné-Bosch S, Garcia QS. ABA and GA(4) dynamic modulates secondary dormancy and germination in Syngonanthus verticillatus seeds. Planta 2020, 251(4):86.
21. Finkelstein R. Abscisic Acid synthesis and response. Arabidopsis Book 2013:e0166.
22. Wang P, Lu S, Zhang X, Hyden B, Qin L, Liu L, Bai Y, Han Y, Wen Z, Xu J et al. Double NCED isozymes control ABA biosynthesis for ripening and senescent regulation in peach fruits. Plant Sci 2021:1–10.
23. Yoshida T, Christmann A, Yamaguchi-Shinozaki K, Grill E, Fernie AR. Revisiting the basal Role of ABA - roles outside of stress. Trends Plant Sci. 2019;24(7):625–35.
24. Wuddineh WA, Mazarei M, Zhang J, Poovaiah CR, Mann DG, Ziebell A, Sykes RW, Davis MF, Udvardi MK, Stewart CN Jr.. Identification and overexpression of gibberellin 2-oxidase (GA2ox) in switchgrass (Panicum virgatum L.) for improved plant architecture and reduced biomass recalcitrance. Plant Biotechnol J. 2015;13(5):636–47.
25. Binenbaum J, Weinstain R, Shani E. Gibberellin localization and transport in plants. Trends Plant Sci 2018, 23(5):410–21.
26. López-Cristoffanini C, Serrat X, Jáuregui O, Nogués S, López-Carbonell M. Phytohormone profiling method for rice: effects of GA20ox mutation on the gibberellin content of japonica rice varieties. Front Plant Sci 2019:1–14.
27. Yamaguchi S. Gibberellin metabolism and its regulation. Annu Rev Plant Biol 2008:225–51.
28. Urbanová T, Tarkowská D, Novák O, Hedden P, Strnad M. Analysis of gibberellins as free acids by ultra performance liquid chromatography-tandem mass spectrometry. Talanta 2013:85–94.
29. Lor VS, Olszewski NE. GA signalling and cross-talk with other signalling pathways. Essays Biochem 2015:49–60.
30. Tuan PA, Kumar R, Rehal PK, Toora PK, Ayele BT. Molecular Mechanisms Underlying Abscisic Acid/Gibberellin Balance in the Control of Seed Dormancy and Germination in Cereals. Front Plant Sci 2018:1–16.
31. Hedden P. Gibberellin metabolism and its regulation. J plant growth Regul 2001, 20(4):317–8.
32. Damaris RN, Lin Z, Yang P, He D. The rice alpha-amylase, conserved regulator of seed maturation and germination. Int J Mol Sci. 2019;20(2):450.

33. Liu Y, Han C, Deng X, Liu D, Liu N, Yan Y. Integrated physiology and proteome analysis of embryo and endosperm highlights complex metabolic networks involved in seed germination in wheat (Triticum aestivum L). J Plant Physiol 2018:63–76.
34. Zhang H, Zhang X, Gao G, Ali I, Wu X, Tang M, Chen L, Jiang L, Liang T. Effects of various seed priming on morphological, physiological, and biochemical traits of rice under chilling stress. Front Plant Sci. 2023;14:1146285.
35. Bakhshy E, Zarinkamar F, Nazari M. Structural and quantitative changes of starch in seed of Trigonella persica during germination. Int J Biol Macromol 2020, 164:1284–93.
36. Hajihashemi S, Skalicky M, Brestic M, Pavla V. Cross-talk between nitric oxide, hydrogen peroxide and calcium in salt-stressed Chenopodium quinoa Willd. At seed germination stage. Plant Physiol Biochem 2020:657–64.
37. Huang Y, Mei G, Fu X, Wang Y, Ruan X, Cao D. Ultrasonic waves regulate antioxidant defense and gluconeogenesis to improve germination from naturally aged soybean seeds. Front Plant Sci 2022:1–12.
38. Wei J, Xu L, Shi Y, Cheng T, Tan W, Zhao Y, Li C, Yang X, Ouyang L, Wei M et al. Transcriptome profile analysis of Indian mustard (Brassica juncea L.) during seed germination reveals the drought stress-induced genes associated with energy, hormone, and phenylpropanoid pathways. Plant Physiol Biochem 2023:107750.
39. Liu R, Lu J, Xing J, Du M, Wang M, Zhang L, Li Y, Zhang C, Wu Y. Transcriptome and metabolome analyses revealing the potential mechanism of seed germination in Polygonatum cyrtonema. Sci Rep. 2021;11(1):1–12.
40. Stark R, Grzelak M, Hadfield J. RNA sequencing: the teenage years. Nat Rev Genet. 2019;20(11):631–56.
41. Liu B, Lin R, Jiang Y, Jiang S, Xiong Y, Lian H, Zeng Q, Liu X, Liu ZJ, Chen S. Transcriptome analysis and identification of genes associated with starch metabolism in Castanea Henryi seed (Fagaceae). Int J Mol Sci. 2020;21(4):1–11.
42. Yu Y, Guo G, Lv D, Hu Y, Li J, Li X, Yan Y. Transcriptome analysis during seed germination of elite Chinese bread wheat cultivar Jimai 20. BMC Plant Biol 2014:20.
43. Zhang H, Chen G, Xu H, Jing S, Jiang Y, Liu Z, Zhang H, Wang F, Hu X, Zhu Y. Transcriptome Analysis of Rice Embryo and Endosperm during Seed Germination. Int J Mol Sci. 2023;24(10):8710.
44. Gao Y, Pan X, Zeng F, Zheng C, Ge W, Sun Y, Du W, Wu X. The identification of suitable internal reference genes in quinoa seeds subjected to abscisic acid and gibberellin treatment. J Seed Sci 2023:e202345034.
45. Chen S, Zhou Y, Chen Y, Gu J. Fastp: an ultra-fast all-in-one FASTQ preprocessor. Bioinf 2018, 34(17):i884–90.
46. Kim D, Langmead B, Salzberg SL. HISAT: a fast spliced aligner with low memory requirements. Nat Methods. 2015;12(4):357–60.

47. Okonechnikov K, Conesa A, García-Alcalde F. Qualimap 2: advanced multi-sample quality control for high-throughput sequencing data. Bioinf 2016, 32(2):292–4.
48. Liao Y, Smyth GK, Shi W. FeatureCounts: an efficient general purpose program for assigning sequence reads to genomic features. Bioinf 2014, 30(7):923–30.
49. Gao Y, Zhang G, Jiang S, Liu Y-X. iMeta : Wekemo Bioincloud: A user-friendly platform for meta-omics data analyses. 2024, 3(1):e175.
50. Li H, Teng K, Yue Y, Teng W, Zhang H, Wen H, Wu J, Fan X. Seed Germination Mechanism of Carex rigescens Under Variable Temperature Determinded Using Integrated Single-Molecule Long-Read and Illumina Sequence Analysis. Front Plant Sci. 2022;3(13):1–13.
51. Han C, Yang P. Studies on the molecular mechanisms of seed germination. Proteom 2015, 15(10):1671–9.
52. MacNeill GJ, Mehrpouyan S, Minow MAA, Patterson JA, Tetlow IJ, Emes MJ. Starch as a source, starch as a sink: the bifunctional role of starch in carbon allocation. J Experimental Bot 2017, 68(16):4433–53.
53. Hao Y, Hong Y, Guo H, Qin P, Huang A, Yang X, Ren G. Transcriptomic and metabolomic landscape of quinoa during seed germination. BMC Plant Biol. 2022;22(1):1–13.
54. Lv Z, Zhu F, Jin D, Wu Y, Wang S. Seed germination and seedling growth of Dendrocalumus Brandisii in vitro, and the inhibitory mechanism of Colchicine. Front Plant Sci 2021:1–12.
55. Crick F. Central dogma of molecular biology. Nature. 1970;227(5258):561–3.
56. Gygi SP, Rochon Y, Franza BR, Aebersold R. Correlation between protein and mRNA abundance in yeast. Mol Cell Biology. 1999;19(3):1720–30.
57. Chick JM, Munger SC, Simecek P, Huttlin EL, Choi K, Gatti DM, Raghupathy N, Svenson KL, Churchill GA, Gygi SP. Defining the consequences of genetic variation on a proteome-wide scale. Nat 2016, 534(7608):500–5.
58. Li M, Wu T, Wang S, Duan T, Huang S, Xie Y. The modulation of sucrose nonfermenting 1-related protein kinase 2.6 state by persulfidation and phosphorylation: insights from molecular dynamics simulations. Int J Mol Sci. 2023;24(14):1–11.
59. Takahashi Y, Ebisu Y, Shimazaki KI. Reconstitution of abscisic acid signaling from the receptor to DNA via bHLH transcription factors. Plant Physiol. 2017;174(2):815–22.
60. Minkoff BB, Stecker KE, Sussman MR. Rapid phosphoproteomic effects of abscisic acid (ABA) on wild-type and aba receptor-deficient a. thaliana mutants. Molecular and cellular proteomics 2015, 14(5):1169–82.
61. Aziz U, Rehmani MS, Wang L, Xian B, Luo X, Shu K. Repressors: the gatekeepers of phytohormone signaling cascades. Plant Cell Rep. 2022;41(6):1333–41.
62. Cui X, Wang J, Li K, Lv B, Hou B, Ding Z. Protein post-translational modifications in auxin signaling. J Genet Genomics. 2023;51(3):279–91.

63. Liu L, Chen J, Gu C, Wang S, Xue Y, Wang Z, Han L, Song W, Liu X, Zhang J, et al. The exocyst subunit CsExo70B promotes both fruit length and disease resistance via regulating receptor kinase abundance at plasma membrane in cucumber. Plant Biotechnol J. 2023;22(2):347–62.
64. Xu J, Yang X, Deng Q, Yang C, Wang D, Jiang G, Yao X, He X, Ding J, Qiang J. TEM8 marks neovasculogenic tumor-initiating cells in triple-negative breast cancer. Nat Commun. 2021;12(1):1–12.
65. Yu F, Wu Y, Xie Q. Precise protein post-translational modifications modulate ABI5 activity. Trends Plant Sci. 2015;20(9):569–75.
66. Brocard IM, Lynch TJ, Finkelstein RR. Regulation and role of the Arabidopsis abscisic acid-insensitive 5 gene in abscisic acid, sugar, and stress response. Plant Physiol. 2002;129(4):1533–43.
67. McGinnis KM, Thomas SG, Soule JD, Strader LC, Zale JM, Sun T-p, Steber CM. The Arabidopsis SLEEPY1 gene encodes a putative F-box subunit of an SCF E3 ubiquitin ligase. Plant Cell. 2003;15(5):1120–30.
68. Mähönen AP, Bishopp A, Higuchi M, Nieminen KM, Kinoshita K, Törmäkangas K, Ikeda Y, Oka A, Kakimoto T, Helariutta Y. Cytokinin signaling and its inhibitor AHP6 regulate cell fate during vascular development. Science. 2006;311(5757):94–8.
69. Kieber JJ, Rothenberg M, Roman G, Feldmann KA, Ecker JR. CTR1, a negative regulator of the ethylene response pathway in Arabidopsis, encodes a member of the raf family of protein kinases. Cell 1993, 72(3):427–41.
70. He J-X, Gendron JM, Yang Y, Li J, Wang Z-Y. The GSK3-like kinase BIN2 phosphorylates and destabilizes BZR1, a positive regulator of the brassinosteroid signaling pathway in Arabidopsis. Proceedings of the National Academy of Sciences 2002, 99(15):10185–10190.
71. Song L, Huang SC, Wise A, Castanon R, Nery JR, Chen H, Watanabe M, Thomas J, Bar-Joseph Z, Ecker JR. A transcription factor hierarchy defines an environmental stress response network. Science. 2016;354(6312):aag1550.
72. Raghavendra AS, Gonugunta VK, Christmann A, Grill E. ABA perception and signalling. Trends Plant Sci. 2010;15(7):395–401.
73. Wu Q, Bai X, Wu X, Xiang D, Wan Y, Luo Y, Shi X, Li Q, Zhao J, Qin P et al. Transcriptome profiling identifies transcription factors and key homologs involved in seed dormancy and germination regulation of Chenopodium quinoa. Plant Physiol Biochem 2020:443–56.
74. Ceccato D, Bertero D, Batlla D, Galati B. Structural aspects of dormancy in quinoa (Chenopodium quinoa): importance and possible action mechanisms of the seed coat. Seed Sci Res 2015, 25(3):267–75.
75. McGinty EM, Murphy KM, Hauvermale AL. Seed dormancy and preharvest sprouting in quinoa (Chenopodium quinoa Willd). Plants. 2021;10(3):1–11.
76. McGinty EM, Craine EB, Miller ND, Ocana-Gallegos C, Spalding EP, Murphy KM, Hauvermale AL. Evaluating relationships between seed morphological traits and seed dormancy in Chenopodium quinoa Willd. Front Plant Sci 2023:1–11.

77. Ritonga FN, Zhou D, Zhang Y, Song R, Li C, Li J, Gao J. The Roles of Gibberellins in Regulating Leaf Development. Plants (Basel). 2023;12(6):1–9.
78. Wang J, Lv P, Yan D, Zhang Z, Xu X, Wang T, Wang Y, Peng Z, Yu C, Gao Y, et al. Exogenous Melatonin Improves Seed Germination of Wheat (Triticum aestivum L.) under Salt Stress. Int J Mol Sci. 2022;23(15):1–9.
79. Kita M, Kato M, Ban Y, Honda C, Yaegaki H, Ikoma Y, Moriguchi T. Carotenoid accumulation in Japanese apricot (Prunus mume Siebold & Zucc.): molecular analysis of carotenogenic gene expression and ethylene regulation. J Agric Food Chem. 2007;55(9):3414–20.
80. Zhang Y, Dai T, Liu Y, Wang J, Wang Q, Zhu W. Effect of Exogenous Glycine Betaine on the Germination of Tomato Seeds under Cold Stress. Int J Mol Sci. 2022;23(18):1–11.
81. Xiao S, Liu L, Wang H, Li D, Bai Z, Zhang Y, Sun H, Zhang K, Li C. Exogenous melatonin accelerates seed germination in cotton (Gossypium hirsutum L). PLoS ONE. 2019;14(6):e0216575.
82. Zheng C, Kwame Acheampong A, Shi Z, Halaly T, Kamiya Y, Ophir R, Galbraith DW, Or E. Distinct gibberellin functions during and after grapevine bud dormancy release. J Exp Bot. 2018;69(7):1635–48.
83. Urbanová T, Tarkowská D, Novák O, Hedden P, Strnad M. Analysis of gibberellins as free acids by ultra performance liquid chromatography–tandem mass spectrometry. Talanta 2013:85–94.
84. Rieu I, Eriksson S, Powers SJ, Gong F, Griffiths J, Woolley L, Benlloch R, Nilsson O, Thomas SG, Hedden P, et al. Genetic analysis reveals that C19-GA 2-oxidation is a major gibberellin inactivation pathway in Arabidopsis. Plant Cell. 2008;20(9):2420–36.
85. Liu Y, Fang J, Xu F, Chu J, Yan C, Schläppi MR, Wang Y, Chu C. Expression patterns of ABA and GA metabolism genes and hormone levels during rice seed development and imbibition: a comparison of dormant and non-dormant rice cultivars. J Genet Genomics. 2014;41(6):327–38.
86. Li Y, Shan X, Jiang Z, Zhao L, Jin F. Genome-wide identification and expression analysis of the GA2ox gene family in maize (Zea mays L.) under various abiotic stress conditions. Plant Physiol Biochem 2021:621–33.

Figures

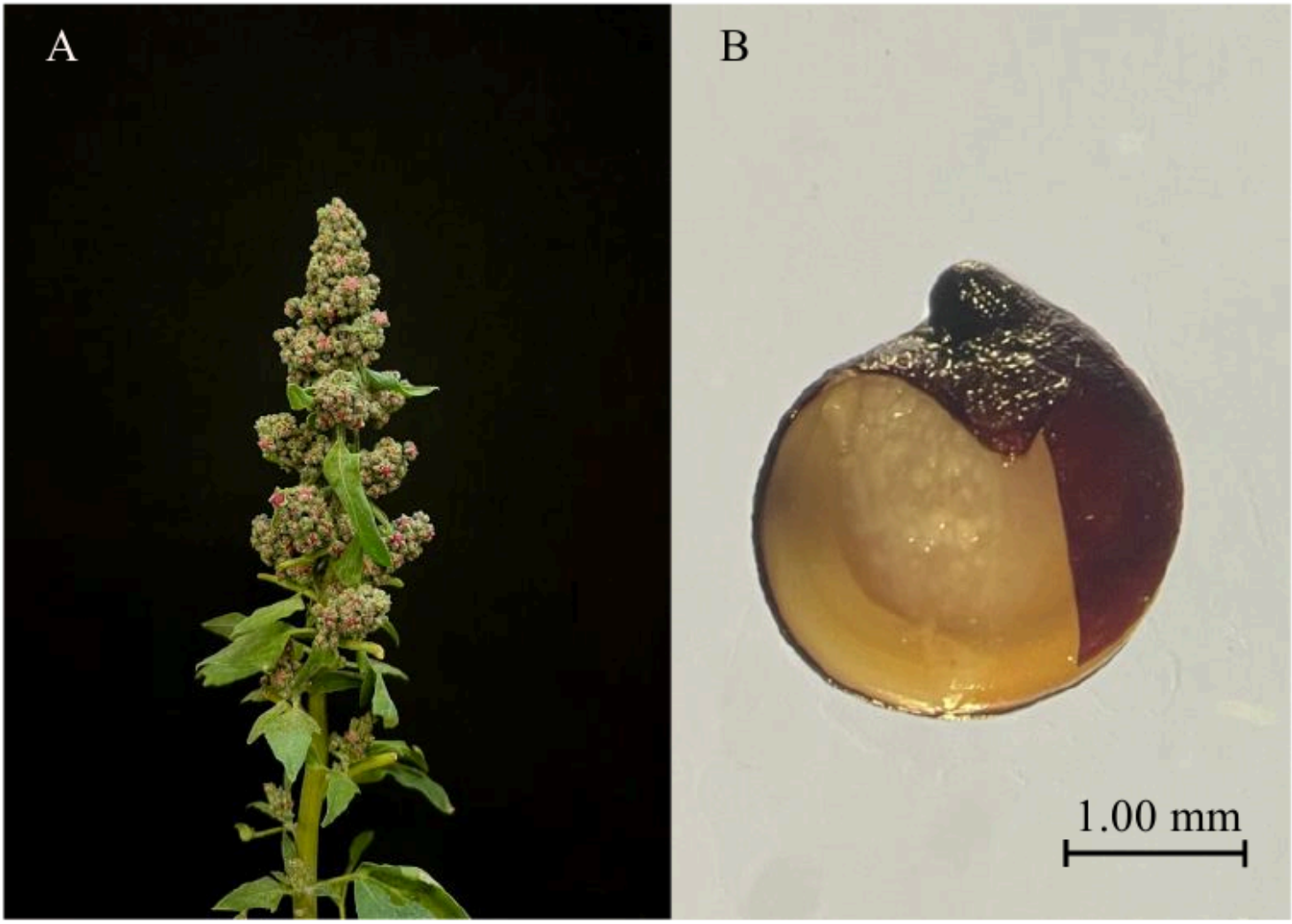

Figure 1

Experimental material CL-2. (A) shows the panicle of the CL-2 plant, while (B) shows the internal morphology of the CL-2 seed. After removing part of the seed coat, it was captured by a stereomicroscope.

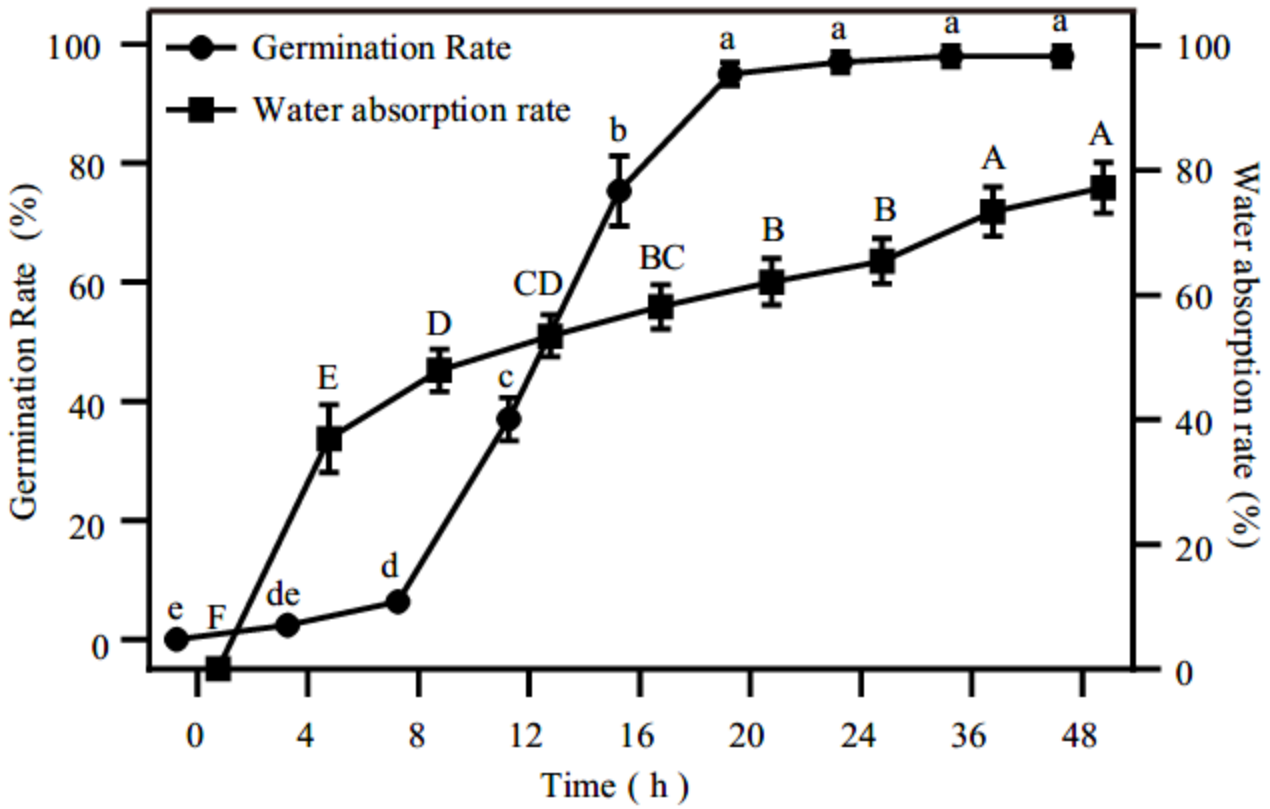

Figure 2

Changes in germination rate and water absorption rate of seeds during germination process.

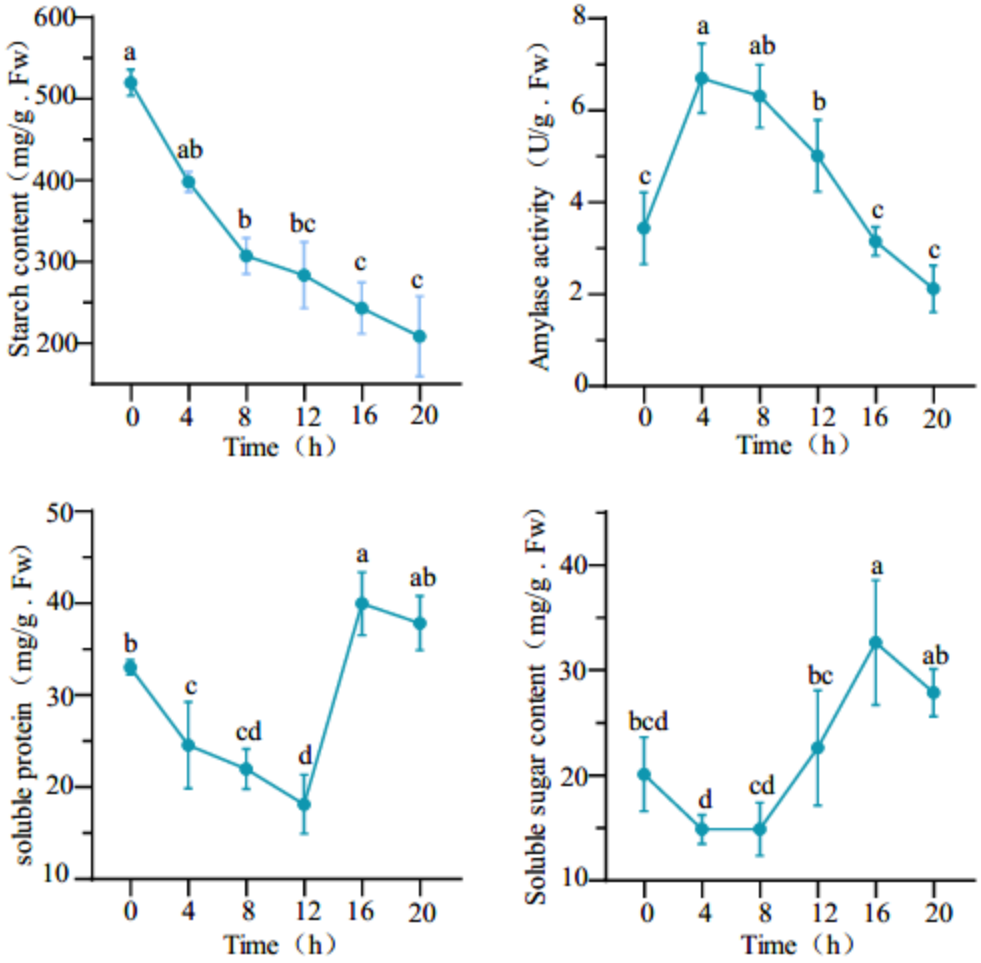

Figure 3

The dynamic changes in physiological and biochemical indicators during the germination process of quinoa seeds.

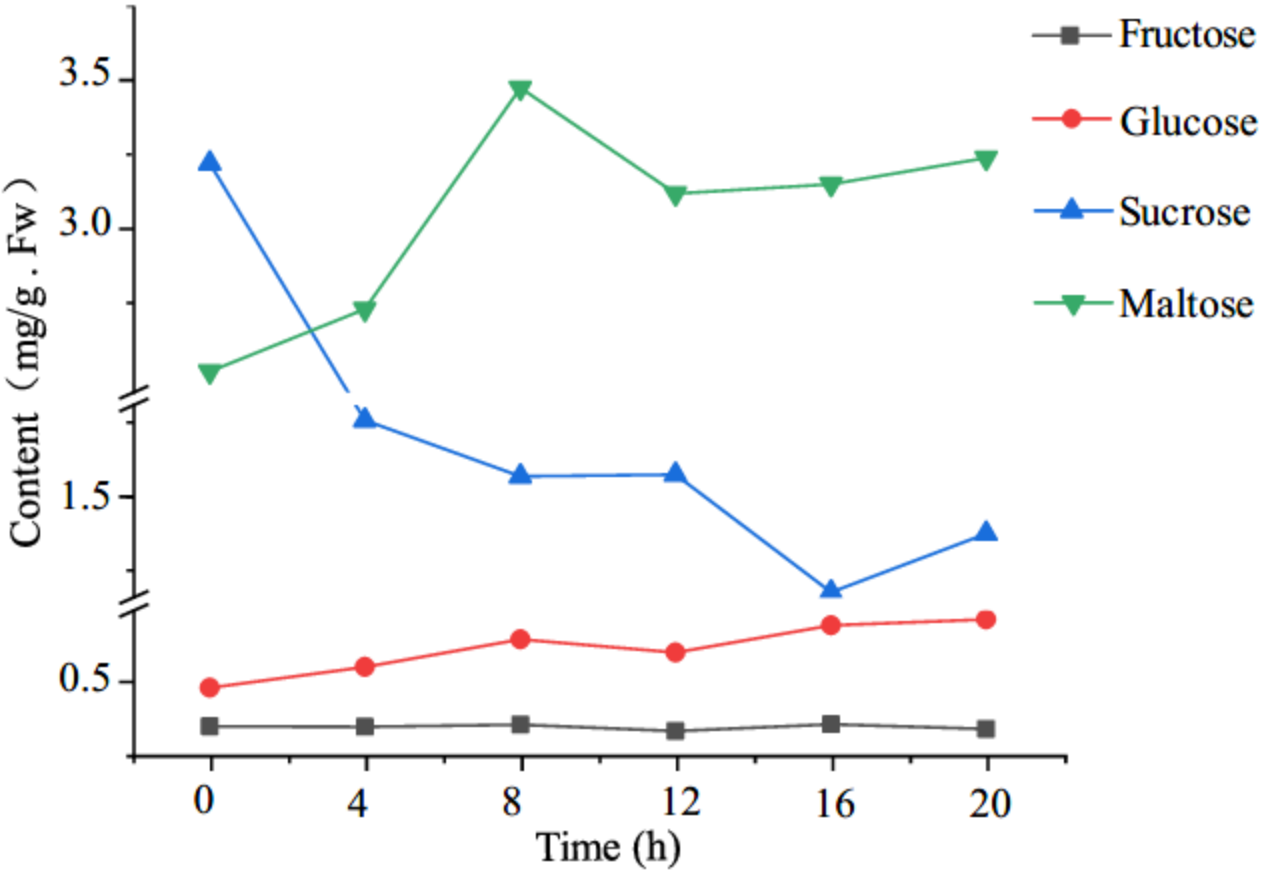

Figure 4

Dynamic fluctuations in the content of low-molecular-weight sugars during the germination of quinoa seeds.

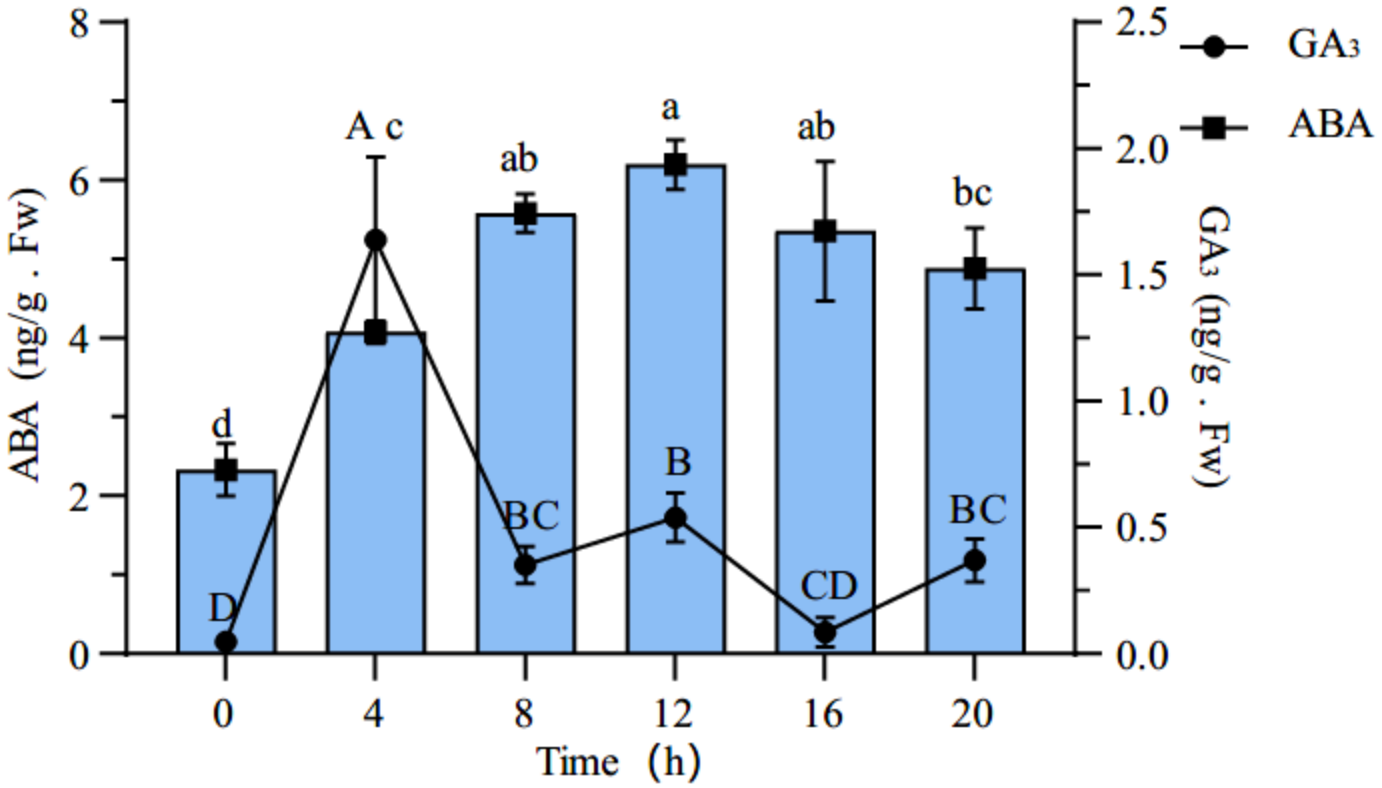

Figure 5

Variations in ABA and GA_3 concentrations throughout the germination process of quinoa seeds. Lowercase letters indicate significant differences in ABA levels based on single-factor analysis ($P < 0.005$), whereas uppercase letters denote significant differences in GA_3 concentrations using the same statistical approach.

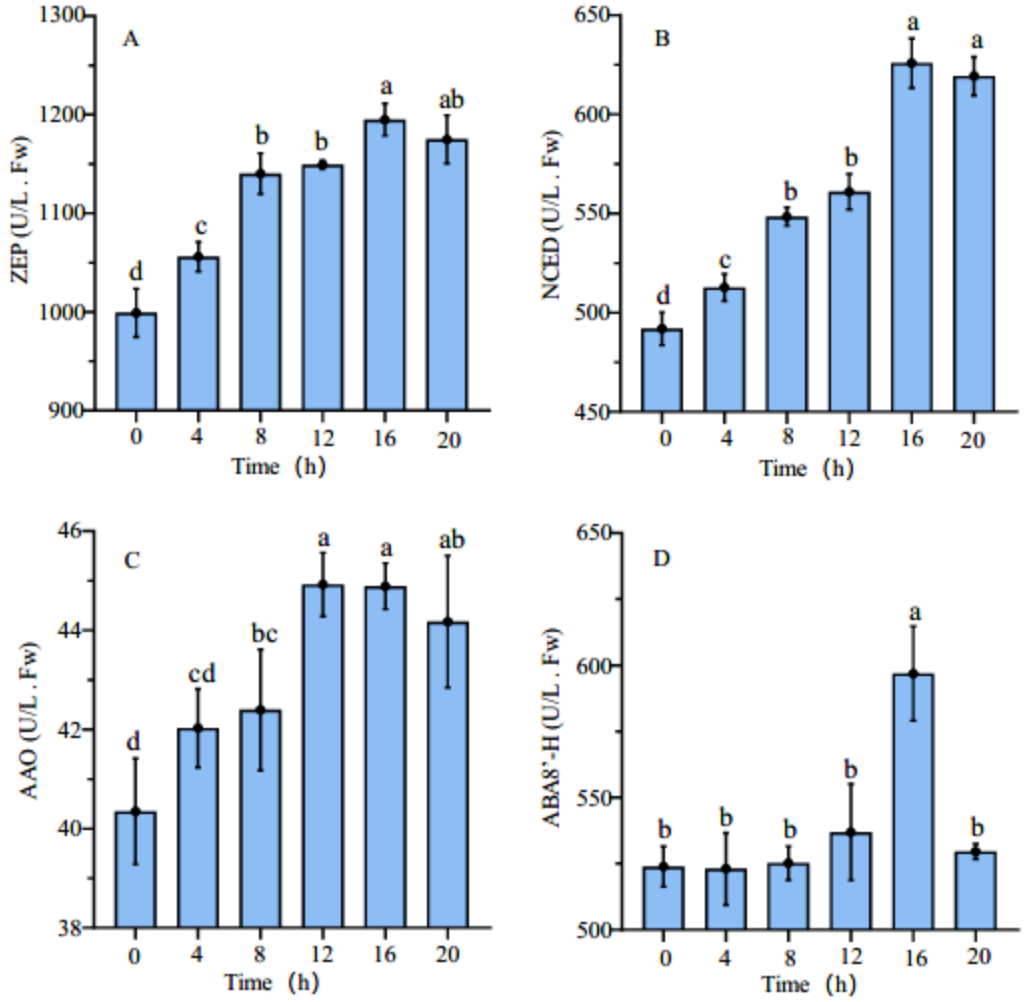

Figure 6

ABA synthesis and metabolic enzyme activity during the germination process of quinoa seeds.

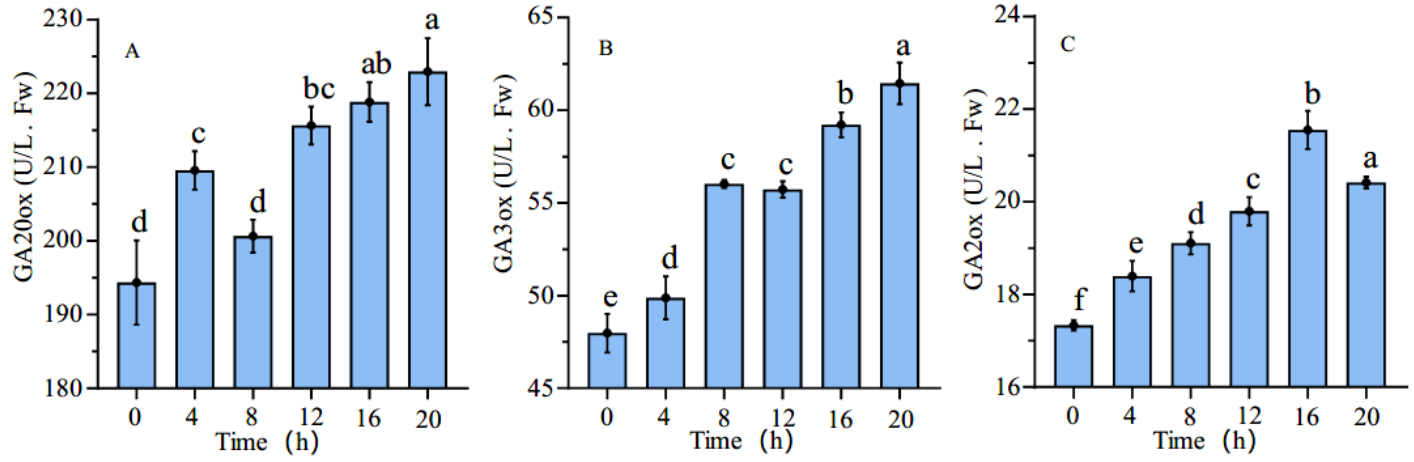

Figure 7

GAs synthesis and metabolic enzyme activity during the germination process of quinoa seeds.

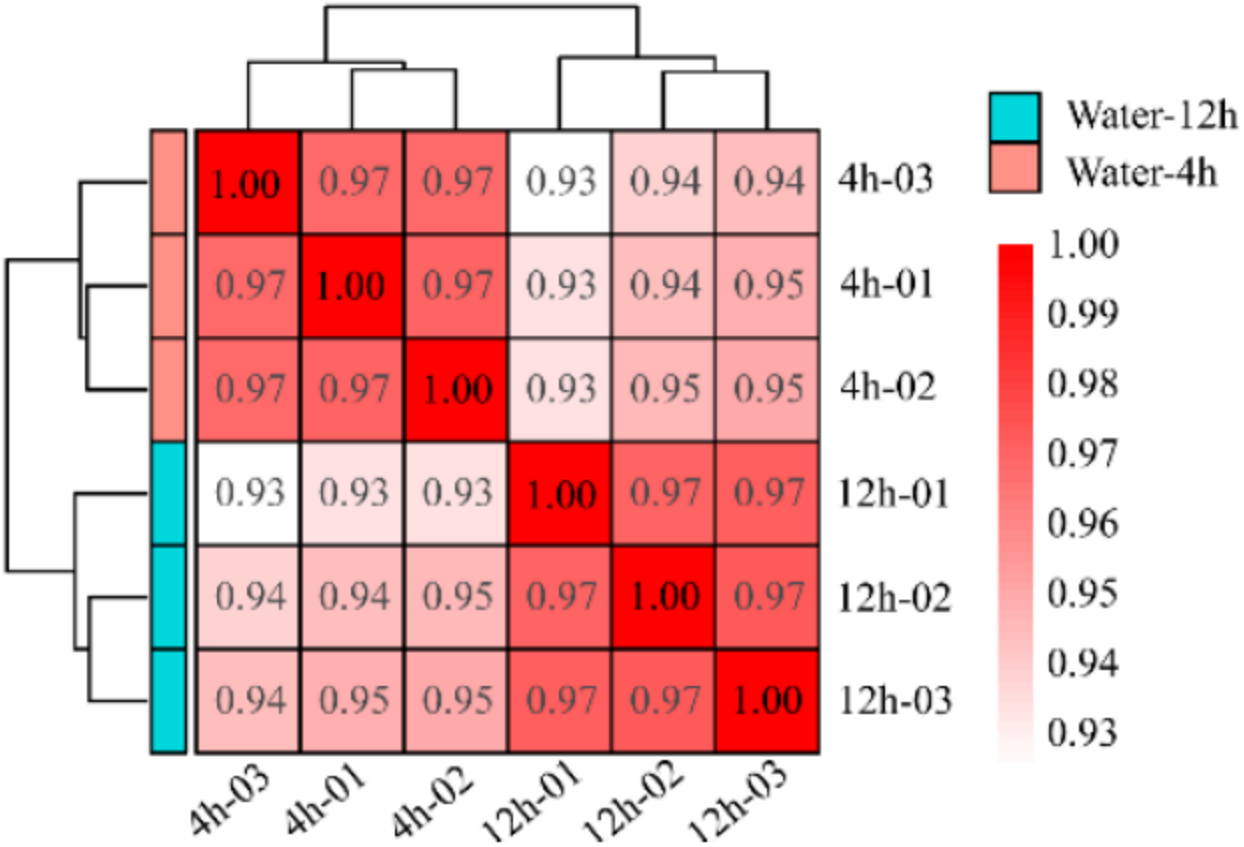

Figure 8

Spearman correlation heatmap between expression level samples.

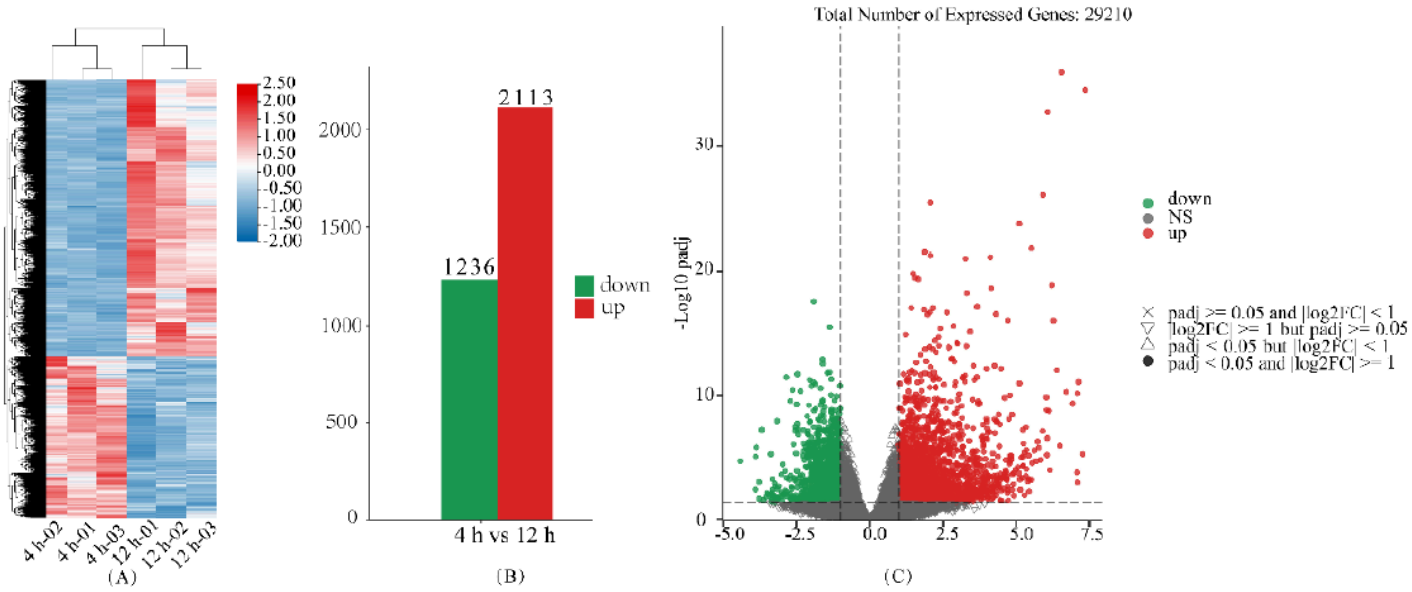

Figure 9

Transcriptome differential gene expression. (A), (B) and (C) represent differential gene analysis expression heatmaps, differential gene analysis summary bar charts, and differential gene analysis volcano charts, respectively.

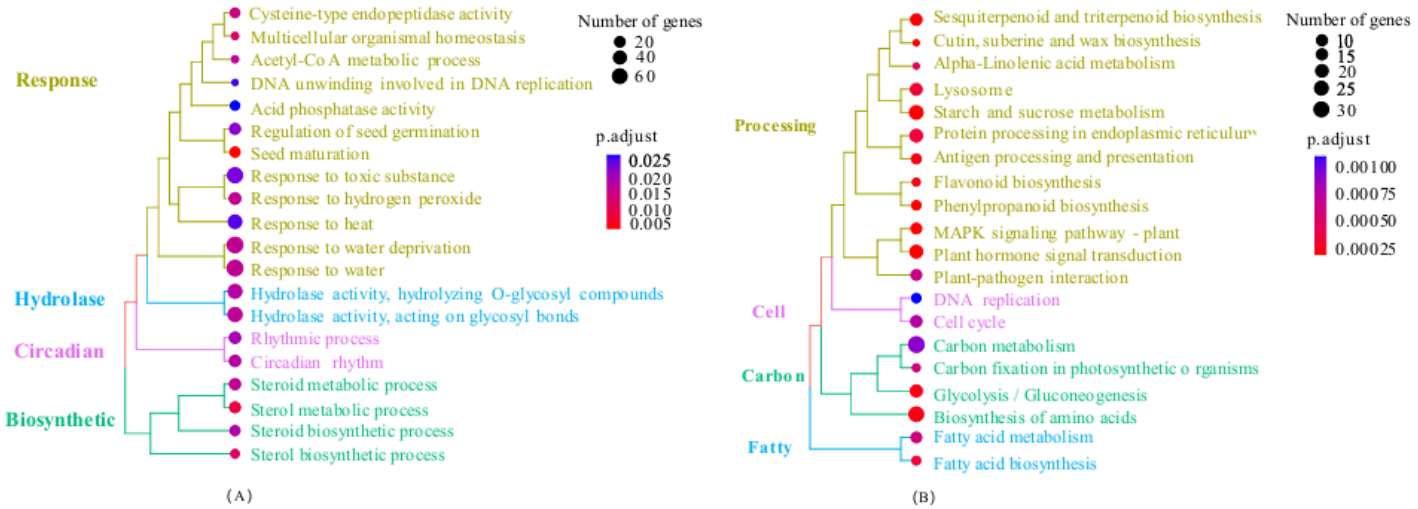

Figure 10

The top 2 significantly enriched pathways of differentially expressed genes. (A) and (B) represent significantly enriched pathways for GO and KEGG, respectively.

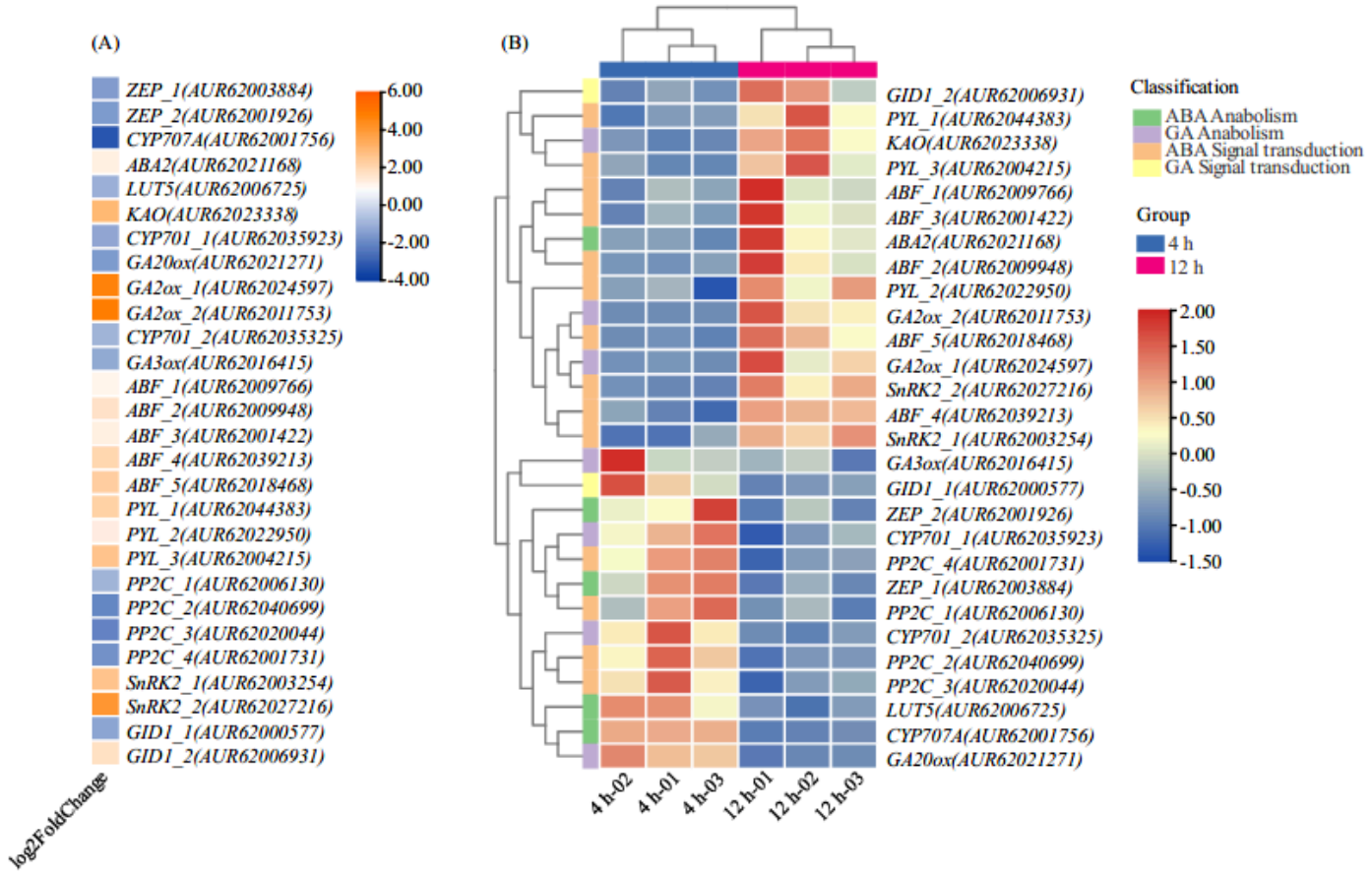

Figure 11

Changes in FPK and FC of ABA and GAs differentially expressed genes.

Figure 12

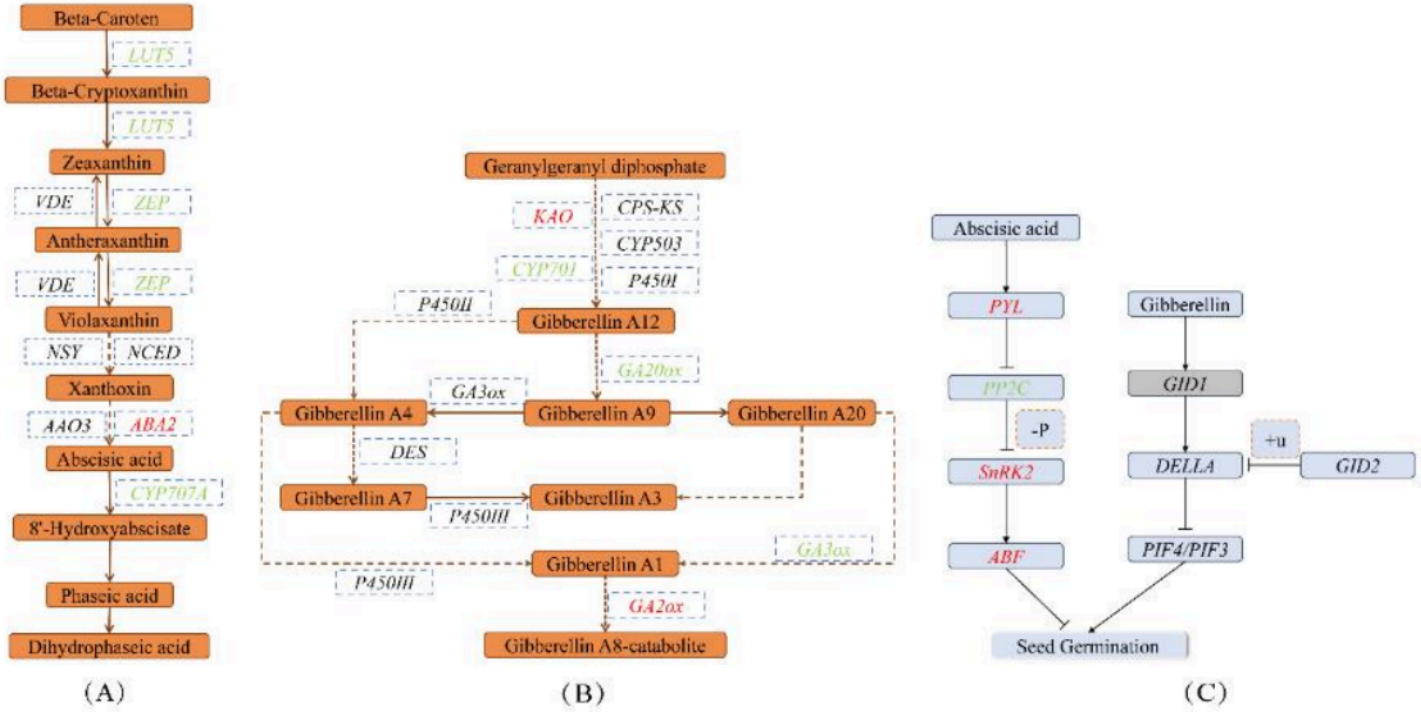

ABA, GAs synthesis and signal transduction pathways. A, B, and C represent the ABA synthesis metabolic pathway, GAs synthesis metabolic pathway, and ABA and GAs-related signaling pathway, respectively. The orange box in the figure represents the compound product, and the dashed box represents the gene involved in this step. The green font represents downregulation, the red font represents upregulation, and the black font represents the gene is not differentially expressed. The gray box filled with black font indicates that among the multiple homologous genes contained in this gene, there are both upregulated and downregulated genes. The dashed line signifies that this step encompasses multiple subprocesses.

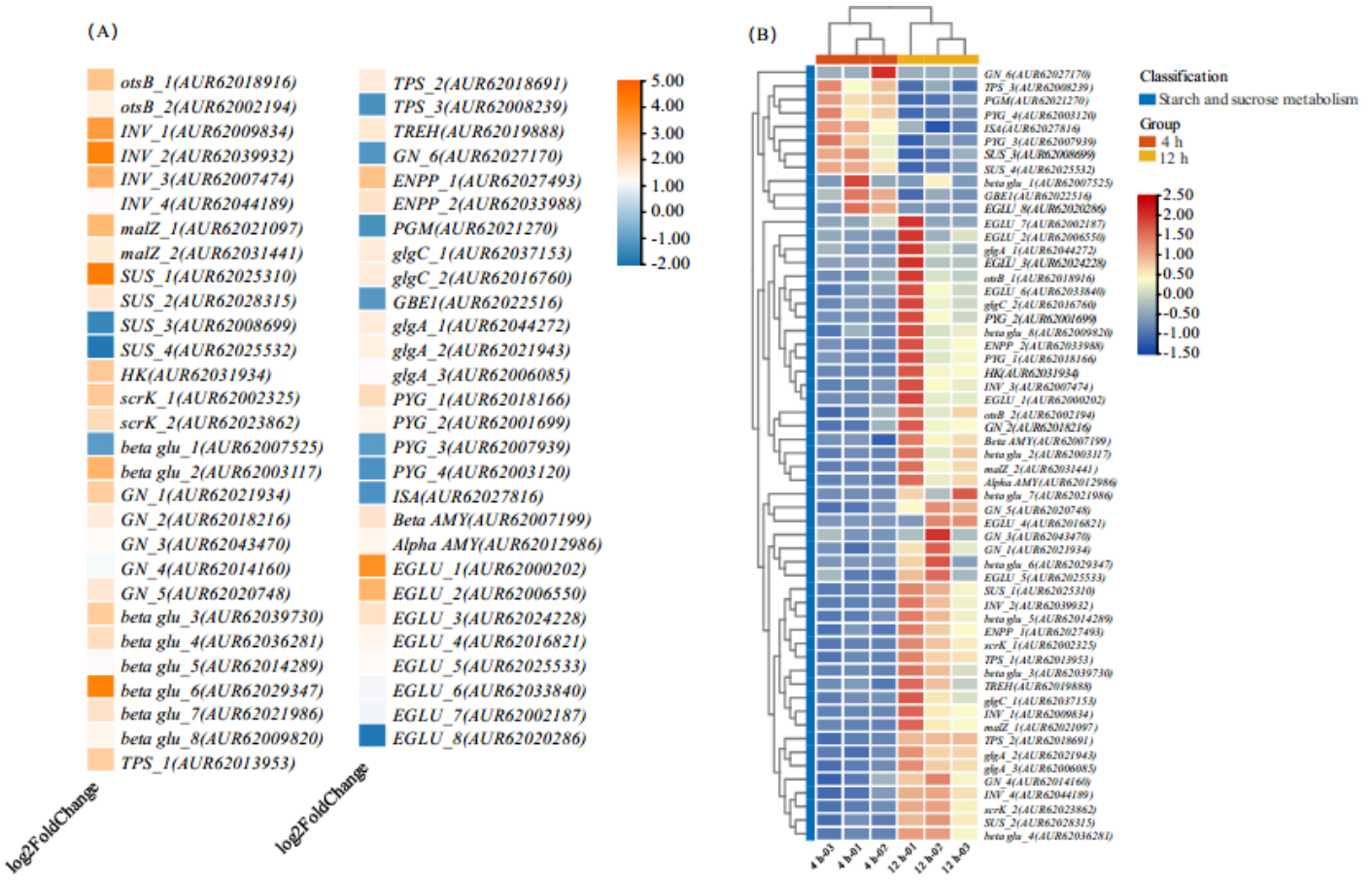

Figure 13

Changes in FC and FPK genes for starch and sucrose metabolism differences.

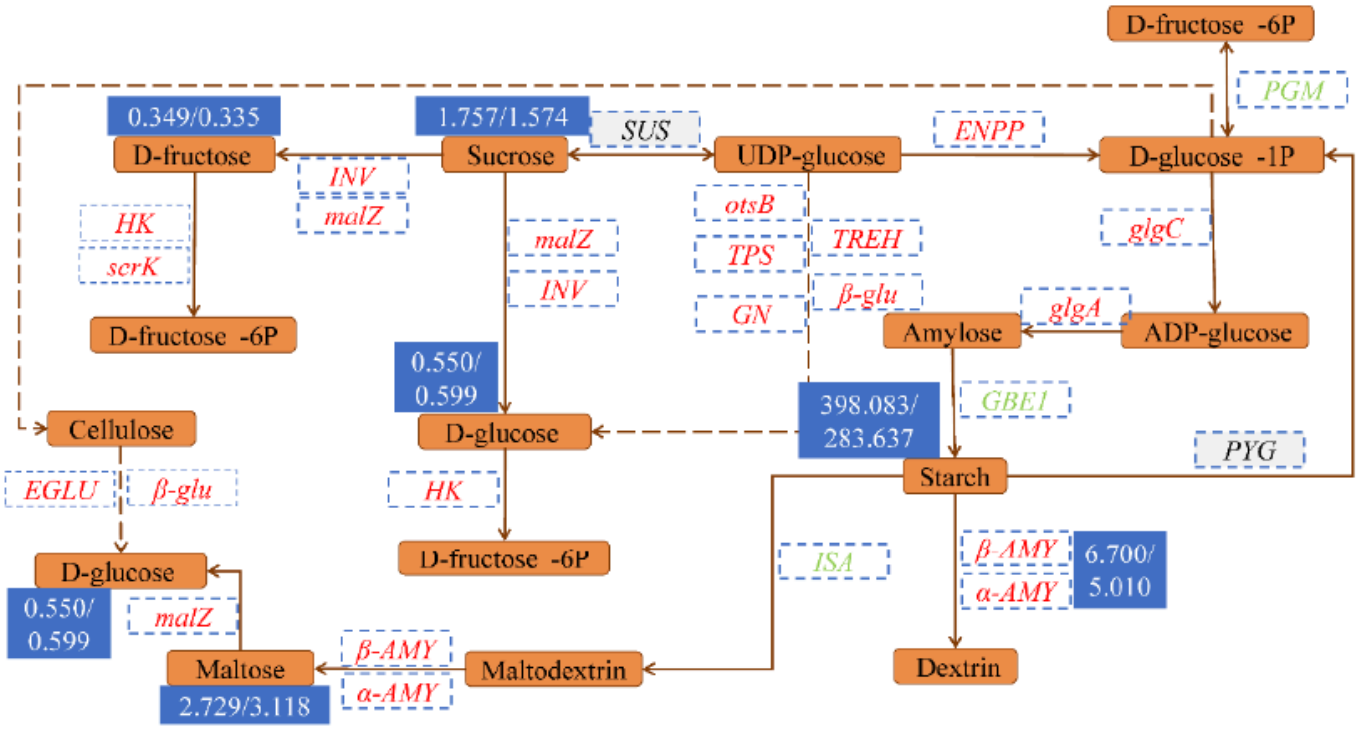

Figure 14

Metabolic pathways of starch and sucrose. The orange box in the figure represents the compound product, and the dashed box represents the gene involved in this step. The green font represents downregulation，the red font represents upregulation. The gray box filled with black font indicates that among the multiple homologous genes contained in this gene, there are both upregulated and downregulated genes. The blue box and white font indicate the content of the product at 4h and 12 h (4h 12 h), The dashed line signifies that this step encompasses multiple subprocesses.

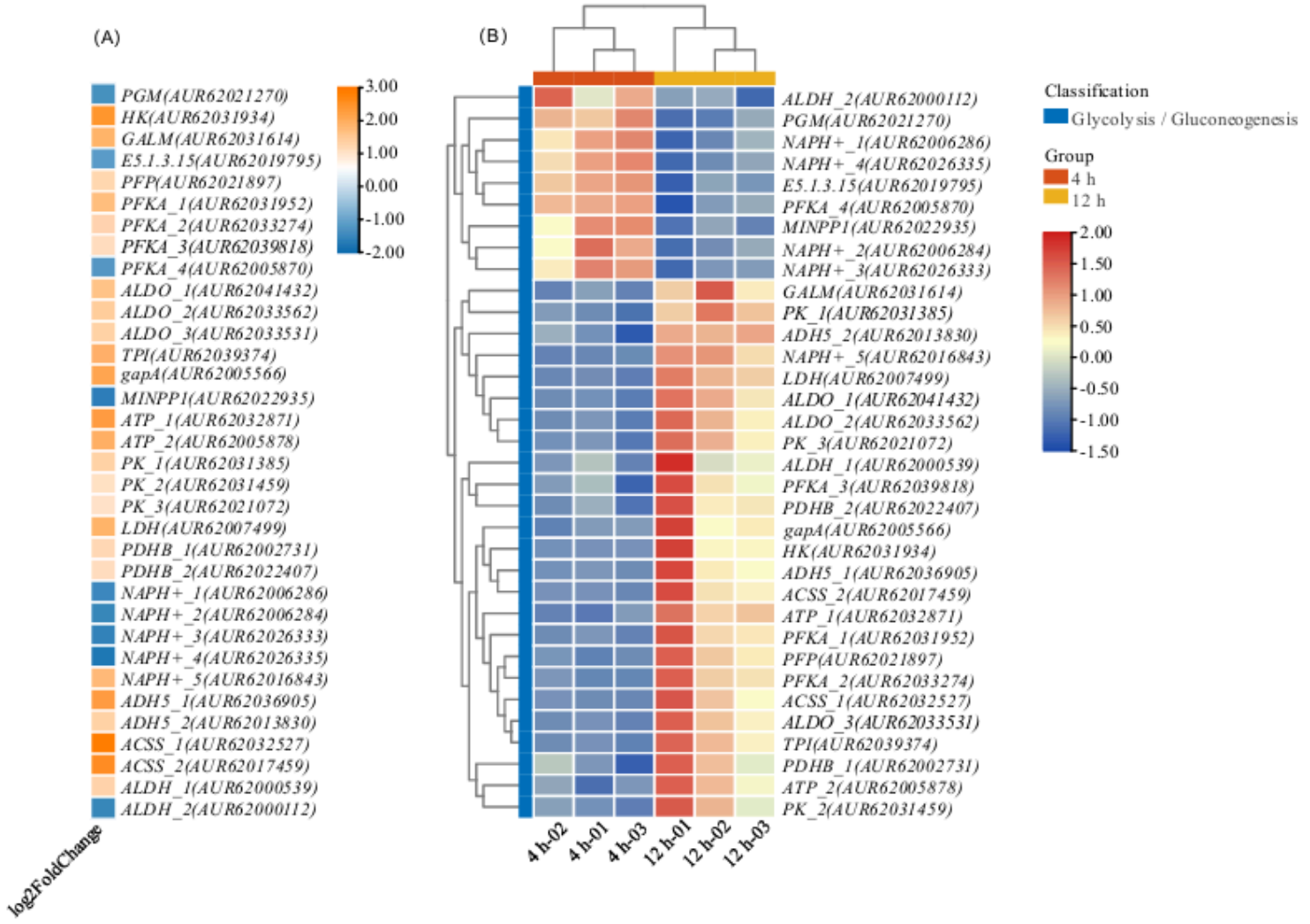

Figure 15

Changes in differential genes FC and FPK in glycolysis.

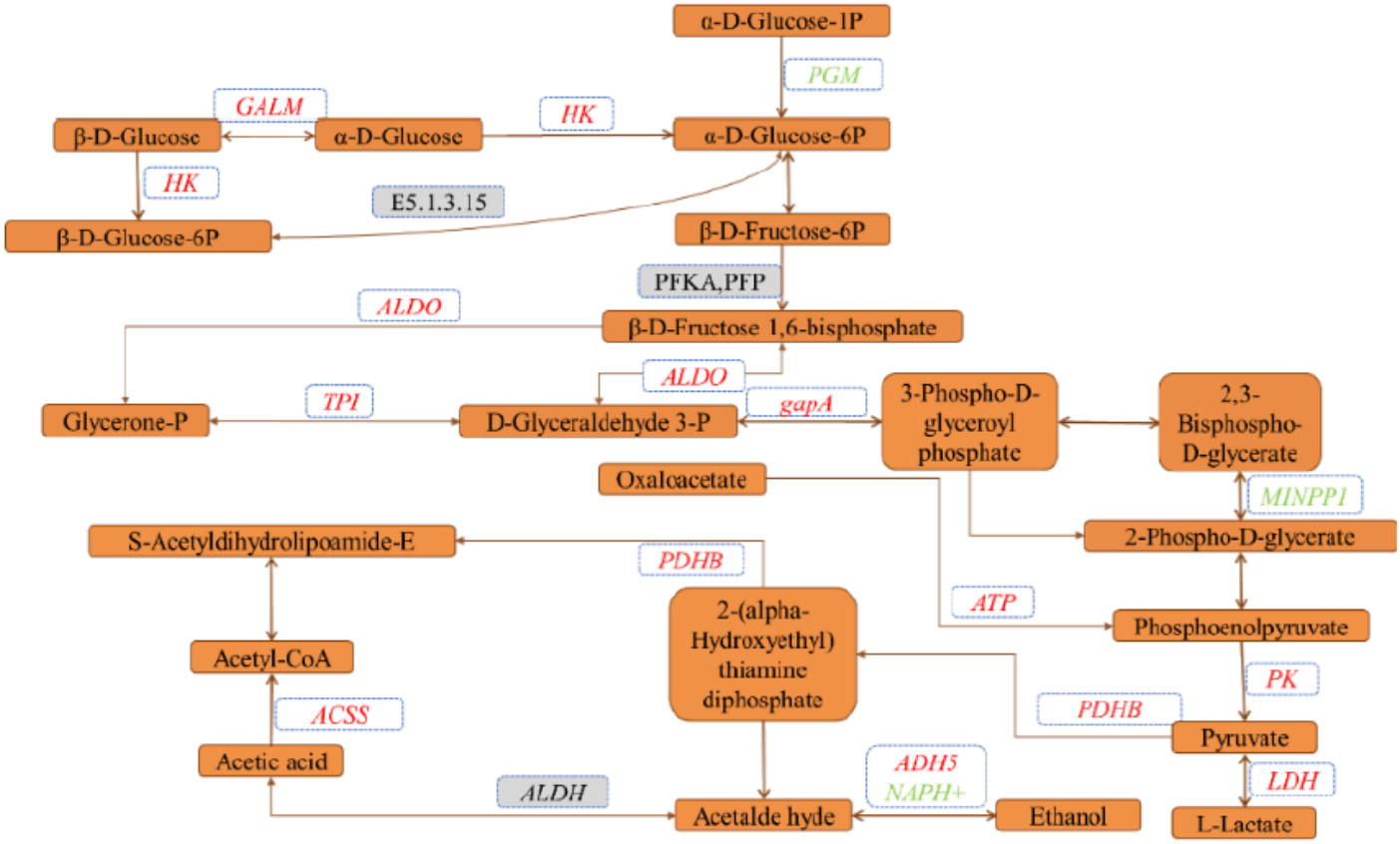

Figure 16

Glycolysis Pathway. The orange box in the figure represents the compound product, and the dashed box represents the gene involved in this step. The green font represents downregulation the red font represents upregulation. The gray box filled with black font indicates that among the multiple homologous genes contained in this gene, there are both upregulated and downregulated genes. The dashed line signifies that this step encompasses multiple subprocesses.

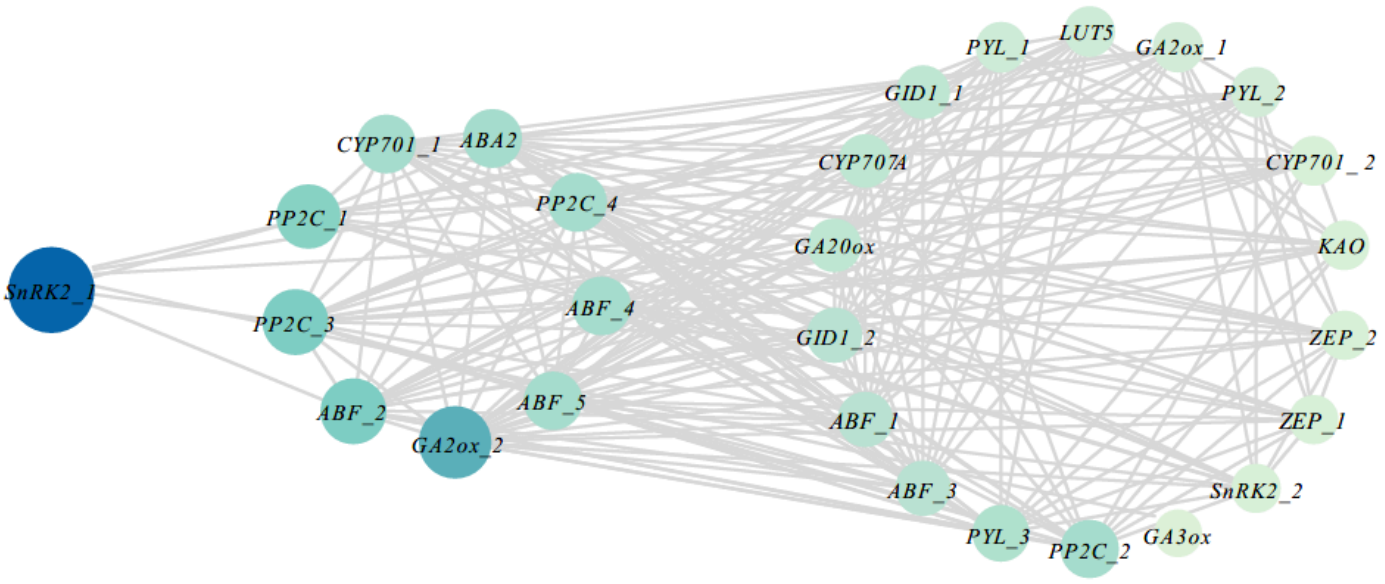

Figure 17

Correlation of differentially expressed genes in ABA and GAs synthesis metabolism.

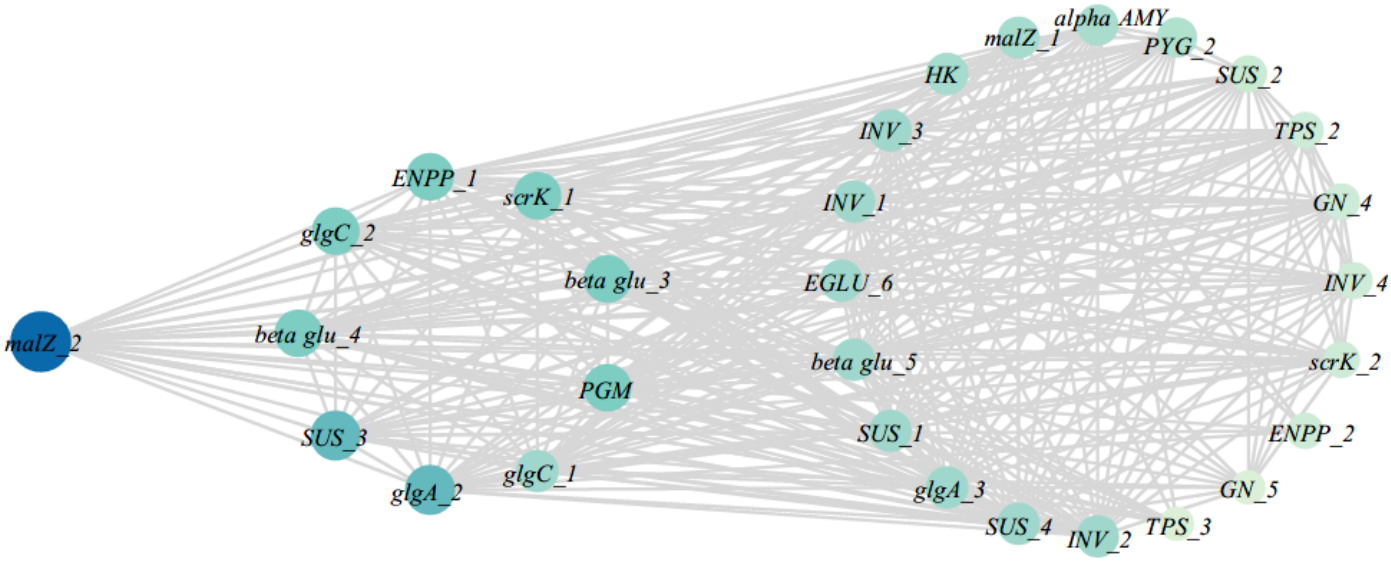

Figure 18

Gene correlation of starch and sucrose metabolism differences.

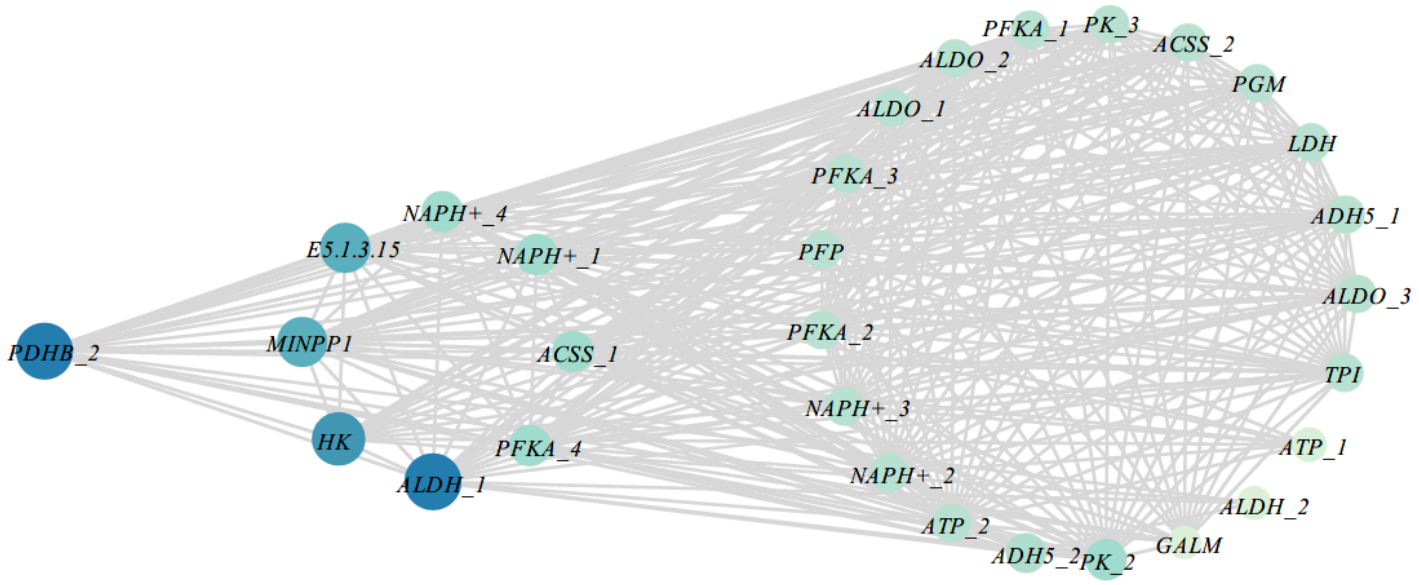

Figure 19

Correlation of differentially expressed genes in sugar metabolism.

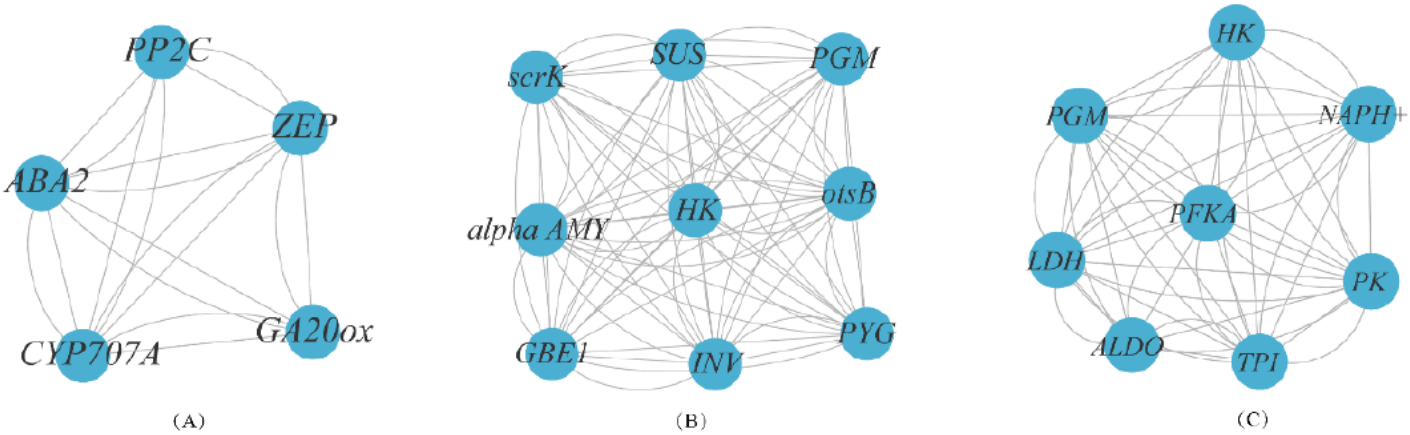

Figure 20

Network diagrams of different path centers. A, B, and C represent ABA, GA metabolism and signaling pathways, starch and sucrose metabolism pathways, and glycolysis pathways, respectively.

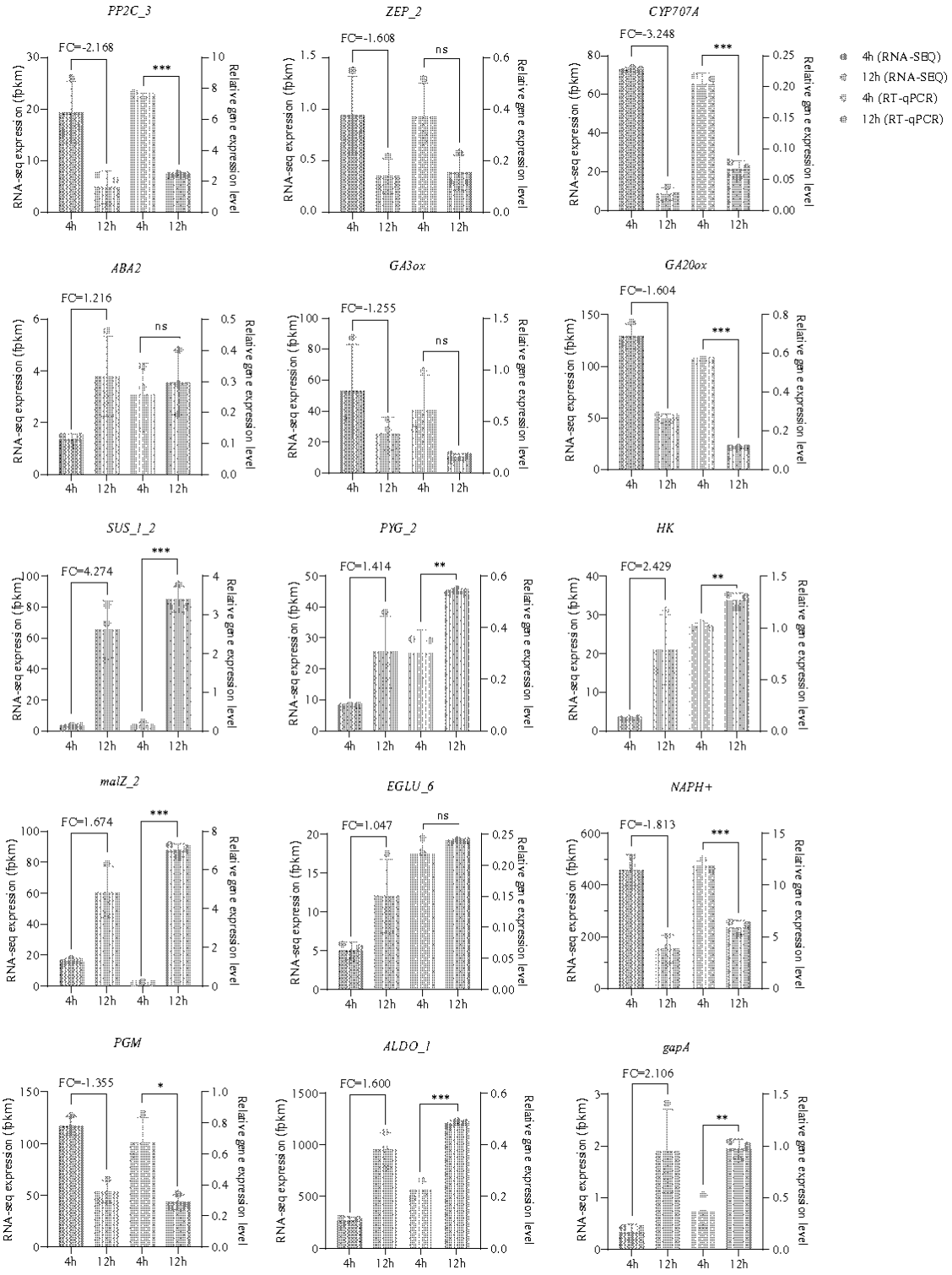

Figure 21

Relative expression levels of 15 genes FPK and RT-qPCR.

Supplementary Files

This is a list of supplementary files associated with this preprint. Click to download.

- Supplementarymaterials.docx